UNIVERSITY OF CALIFORNIA

SANTA CRUZ

THE CENTRAL REGION OF THE CELLULAR PRION PROTEIN ATTENUATES THE INTRINSIC TOXICITY OF N-TERMINUS

A dissertation submitted in partial satisfaction
of the requirements for the degree of

DOCTOR OF PHILOSOPHY

in

CHEMISTRY

by

Graham P. Roseman

December 2019

Thesis Dissertation of Graham P. Roseman
is approved:

_____
Professor Seth M. Rubin, Chair

_____
Professor Glenn L. Millhauser

_____
Professor William G. Scott

_____
Quentin Williams
Acting Vice Provost and Dean of Graduate Studies

Table of Contents

List of Figures

Chapter 1

Chapter 2

Chapter 3

ABSTRACT

The Central Region of the Cellular Prion Protein Attenuates the Intrinsic Toxicity of N-Terminus

Graham P. Roseman

The misfolding of the cellular prion protein (PrP^{C}) into the aggregate prone conformer (PrP^{Sc}) is at the heart of a class of neurodegenerative diseases called transmissible spongiform encephalopathies (TSEs). These diseases affect humans, bovine, sheep, and other mammals. PrP^{C} is a well conserved mammalian protein and is highly expressed in the brain. PrP^{C} is composed of two main domains consisting of the unstructured N-terminus and the structured C-terminus. The two main domains are connected by a short linker called the central region (CR). Previous studies have shown internal amino-proximal deletions spanning the CR generate a profound neurotoxicity in mice. The toxicity generated by these deletions have been shown to parallel bona fide prion diseases, and thus making them a good model system for studying prion diseases. The neurotoxicity elicited by CR deletion mutants is thought to originate from a misregulation of the extreme N-terminus of PrP^{C}. However, these deletion mutants make two major changes that could potentially lead to the misregulation of the N-terminus. These include: 1) weakening of a protective metal-

driven *cis*-interaction, and 2) deletion of the locus important in a regulatory cleavage event. This study used designed mutations to allow for one of these changes at a time while not altering the other. We find that neither blocking the metal-driven *cis*-interaction nor cleavage generates toxicity. Conversely, we show that the WT PrP^C CR sequence is necessary for regulating the toxicity. Moreover, we find that the WT PrP^C CR sequence is necessary for PrP^C homodimerization on the cell surface, which could be a protective mechanism from the deleterious effects of a misregulated extreme N-terminus. Additionally, we found that pathological mutations in the CR causing a certain set of prion diseases in humans do not affect the metal-driven *cis*-interaction. Furthermore, these result suggests a difference in the origin of neurotoxicity between CR pathological mutations and C-terminal pathological mutations.

For

My Parents

Acknowledgements

First and foremost, this dissertation is about the science and the endeavor to uncover its beauty using research as the tool. To undertake that honor, it was only possible by funding systems, for us that is the National Institute of Health, and a home for laboratories, for us that is UCSC, to work hard to uncover its magnificence. This research would not have been possible without the help of multiple labs, numerous collaborations, late night discussions, patient friends and family willing to work with me to help push the field further.

As a young researcher, I would have been nothing without the help of my advisor Glenn Millhauser. He invested his time, interest, and money to allow me to evolve into the independent researcher I am today. His patience and guidance permitted me to figure out what works, what does not work, and how much time it is worth spending on something that just may never work. Additionally, his writing skills have been an incredible influence on me. This taught me to not only be able to communicate the highly complicated language of chemistry and biochemistry, but how to communicate to an audience that does not have any scientific background. For all of this and more, I am forever grateful.

I would also like to thank my committee, Dr. William Scott and Dr. Seth Rubin. Seth has always been available for me to walk into his office and ask almost anything, from research to life after graduate school. William was also always interested in a

scientific discussion. Additionally, I taught multiple quarters of undergraduate biochemistry with William. During this time, I learned a style of teaching that I will always keep. He taught me to not just teach them the homework or how to pass the class by knowing all of the answers, but rather teach them the contents and teach them how to arrive to the answer using intuition.

I would also like to thank Dr. Carrie Partch and Dr. Michael Stone. Carrie is one of the most brilliant researchers I have ever met. She not only runs a huge lab at UCSC, she also is a fantastic source of knowledge on what to do after graduate school. Michael is a great resource as well. Having taken a graduate biochemistry course with him, and as well as taught undergraduate biochemistry with him, I've learned to be very critical of every experiment I do. He always challenged me by asking "why do you think this is the best experiment" and "what are the drawback of this technique". These are major questions asked that have shaped me into the critical scientist I am today.

I want to thank all of field experts who helped me throughout the years in graduate school. Dr. Jack Lee was instrumental in teaching me how to use the NMR and how to analyze the data. He also made sure that every experiment I did was thought out and worth the time doing it. Eefei Chen helped me learn circular dichroism for one of my first projects I came up with in graduate school.

I also want to thank music for helping me survive graduate school. Going to punk and emo and hardcore shows at my YMCA, as well as playing some of those

shows, in my hometown as a teenager has really shaped me. If you have seen me walking down the halls, I'm usually blasting music through my head phones and jamming out. Playing guitar has also been my therapist. There is nothing like getting home from the lab and just going at it on the guitar. For that, I am thankful.

My success in graduate school cannot just be equated to fantastic mentorship. A large part is the result of having an amazing group of lab mates who foster an environment that I thrived in. Valerie Chen and I joined the lab at the same time and we kicked it off due to our shared love of emo music. Even though the biological system we researched was different, we were able to push each other scientifically. It has also been a pleasure to see her grow into the amazing scientist that she is today. Dr. Eric Evans was the one who taught me almost everything I know about EPR. He was one of the most meticulous experimentalists I've ever met. The most important lessons he ever taught me was, in his words, "Just put it in a tube". That simple lesson led to multiple publications that ranged in topics from material science to protein biochemistry. Dr. Rafael Palomino was my mentor when I first rotated in the lab and showed me the independence we get in the Millhauser lab, which was a big factor with me joining this research group. Additionally, Rafael and Eric introduced me into the world of good coffee, which is something I will enjoy throughout my entire life. Dr. Kate Markham was one year above me and we worked on a similar aspect of the prion protein. Even though we butted heads at times, she was like the older sister I never had, and it was a pleasure to work with her. Kevin Schilling joined two years

after me and immediately turned into the “fixer-of-everything” in our lab. It was cool to help form his first project, which he has ultimately taken to a completely new level and will get a few very good publications from it. The newest graduate student in the lab, Mark Wadolkowski, helped me with an important experiment in my main manuscript. I’ve really enjoyed our talks about guitar and metal music. Dr. Tufa Assafa was the newest person to join the lab, and I really appreciated his expert insight into EPR experiments I was running for my collaborators. I really want to thank all you for dealing with me and my eccentricity and my loud whiney emo music. You have all made a tremendous impact on me and my life and I truly cannot begin to thank you all enough.

Since being in the Millhauser lab, I’ve found out that I really love to mentor students. I’ve luckily have had my share of wonderful undergraduate students work for me. The first of these undergraduates was Nathan Peterson. He was an extremely energetic and motivated student who helped during the time I conceived my main doctoral research project. He also helped teach me quickly that mentoring is something that I love. Roman Reggiardo was my second student and proved to learn quick. His intelligence helped him push his project far in addition to helping others in the lab on their projects. Ultimately he joined a graduate program at UCSC and is doing fantastic. Taylor Schumann was a great undergrad who helped me on a few projects before she transferred to UCSD. Julia Martin was my last undergraduate that I mentored. Her and I shared a love for music and sarcasm. If anyone can out sarcasm

me, she can. This light side to her did not take away from her brightness and motivation to achieve. It was amazing to see her grow as a researcher. This growth led her to a graduate program at Berkeley. I want to thank all the undergraduates I mentored. I hope I was as inspirational to you all as you all were to me.

As much as science is a huge part of my life, I need to have a life outside of the lab. Since I moved to California from the greater Philadelphia area across the country, I had to meet people. Luckily my first neighbors took me under their wings and we are still amazing friends. Two years into graduate school, I moved into an amazing house of graduate students. I am thankful for all of the deep conversations, late nights staying up after a long day of research, the parties, the occasional one too many beers, and the countless number of fun times we've had together as a community. I've got to watch them all grow and they were able to watch me grow as well. We will be friends until the end, and for that I am grateful.

Other than my Santa Cruz friends, I would not be who I am today without my best friends Tom Rose and Chris Mezick. Tom and I met in Mrs. Howard's class in first grade. We instantly became best friends, which has lasted for over twenty years. We met Chris in middle school and we all became best friends. We played in bands together. We did stupid things together. I had their backs, and when my parents split up, they sure as hell had mine. I still talk to Tom at least one to two times every two to three weeks despite me being in California and him being in Pennsylvania. Real

quick, all good. They will always be my best friends for life. Thank you and I love you both.

Of course none of this would be possible without the help and patience that my parents constantly give to me. My mom was an analytical chemist at Johnson and Johnson for over 25 years. The fact that she just had an associate's degree and was a chemist is probably the most influential reason for why I thought it was a good idea to get a PhD. I still think it was a good idea. My dad got into programming in the 1990's, which was perfect for the way his brain works. He taught me patience and kindness and love. My dad and I got very close when my parents separated. He will always be my biggest fan, which is amazing. I love my parents, hence this dissertation is dedicated to both of you. Thank you for life.

CHAPTER 1

Introduction

Recognizing a New Disease

During the 1700's in England and throughout Europe, wool was viewed as a highly valuable and economically desirable commodity, thus making shepherds an integral part of society [1]. However, in 1732, shepherds began getting concerned after observing a new illness occurring in their two to five-year-old sheep. Typically, symptoms were initially presented as subtle changes in behavior and temperament. Next, the affected sheep would begin to scratch themselves and rub against fence posts to alleviate a seemingly unrelievable itch (Figure 1).

Figure 1: **Sheep displaying sings of scrapie**. The loss of wool due to profuse scratching is a characteristic sign that this sheep has scrapie [2].

Eventually after approximately six months, the majority of the sheep's wool would be scraped off. This became a defining trait of the disease, ultimately leading to naming the disease scrapie. As the disease progressed, the sheep developed uncoordinated movements and an altered gait. Approximately six months after symptom onset, the sheep would inevitably perish. Finally, in 1755, the British parliament began discussions regarding this emerging disease and the imminent economic impacts it would have on society [3]. This initiated the written history of scrapie, and ultimately a new class of diseases.

Scrapie began emerging in other European countries, eventually leading to discussions in Germany in 1959 with respect to how the government would handle this impending epidemic. The German veterinarian, J.G. Leopoldt, stated that once a shepherd recognized a sheep had scrapie, they must "…isolate such an animal from healthy stock immediately because it is infectious and can cause serious harm to the flock." [1]. This statement significantly first described scrapie as an infectious disease.

During the middle of the 19th century, veterinarians throughout Europe began scientifically investigating scrapie with the hope of understanding the disease pathology, transmission, and the infectious pathogen. In 1898, from post-mortem analysis of scrapie infected brains, Besnoit and colleagues recognized neurodegeneration as a prominent neuropathological characteristic of the disease [4], which explained the neurological symptoms such as loss of coordination and gait abnormalities. Moreover, these observations implied that the disease may be

neurological in origin. Intriguingly, even though it was known that scrapie was transmitted from sheep to sheep, Besnoit and colleagues were unable to experimentally transmit scrapie from one sheep to another sheep via blood transfusion or direct brain inoculation [5]. However, in 1936, after noticing that epidemiological studies suggested naturally occurring scrapie has an incubation period of 18 months or longer, Cuillé and Chelle successfully transmitted scrapie to two healthy sheep [6]. Notably, they determined the incubation period is significantly longer than other transmissible diseases, which implied a novel property of the scrapie infection.

Right around the time of the Cuillé and Chelle transmission experiments in 1935, a vaccine for the looping-ill virus was developed and administered to roughly 18,000 sheep [7]. This resulted in a scrapie outbreak two years later in 1937. It was later determined that one of the batches of the vaccine was prepared from the brain, spinal cord, and spleen of scrapie infected sheep. Overall, the experiments conducted in the 1930s unambiguously defined the transmissible and infectious nature of scrapie.

People Eating People: Kuru

On the other side of the world, in the developing nation of Papua New Guinea, a new disease affecting the Fore people was initially observed by the westerner Ted Ubank in 1936 [8]. Subsequently, western travelers to Papua New Guinea observed

the Fore tribe practicing ritualistic endocannibalism on the deceased. They witnessed that the men would typically dine on the choice cuts from the deceased and the woman and children consumed the leftovers, which included the brain matter and spinal cord meat. Maybe it was just a coincidence that the population who feasted on the brain, being the woman and children, were the ones primarily acquiring the disease. Conversely, it is feasibly imaginable that the brain matter contained an infectious entity that was the driving force of this illness.

In the early 1950s, scientist began to monitor the disease that natives were calling kuru, meaning trembling from fever or cold [9]. The physician Vincent Zigas arrived in Papua New Guinea in 1955, followed by Carleton Gajdusek two years later, to observe and study the etiology of kuru. They recognized that kuru patients had very consistent symptoms starting with ataxia and followed by the occurrence of tremors and jerks [10]. Eventually the patients lost the ability to walk, became bedridden, and ultimately were unable to feed themselves. Intriguingly, kuru patients appeared to be conscious, but they could not express themselves. However, even though patients lacked the ability to verbally express themselves, their faces contained an inappropriate euphoria about their disease and they would compulsively laugh. This influenced the media to call the disease “laughing death” (Figure 2).

Figure 2: **Children affected with Kuru**. The boy on the left and the boy on the right are unable to stand on their own. They also have a euphoric glow to them, even though they will be dead within a year [11].

Unfortunately, kuru is always fatal approximately 12 months after symptom onset. Remarkably, even though the exact origin of the kuru etiology was unknown, the assumption that the practice of ritualistic endocannibalism triggered the disease was made. This would not be formally proven until the 1980s by Robert Klitzmann, who published a study that followed kuru patients who participated in only a few number of feasts of the disease ridden deceased [12]. Ultimately, when the practice of endocannibalism ceased by the Fore people, the rate of kuru declined.

Similar to scrapie, the ataxic symptoms and the occurrence of tremors in kuru patients suggested to researchers that kuru is neurological in origin. Intriguingly, the brain of kuru patients appeared macroscopically similar to a healthy brain [11]. This

led Zigas and Gajdusek to send brain slices to Igor Klatzo at the National Institutes of Health (NIH) to view under the microscope. Klatzo observed massive neurodegeneration and neurophagia in the brain slices [13]. Vacuolization and spongiform was apparent in the striatum, a region that facilitates voluntary movement, and in the cerebellum, which relays sensory information to regulate motor movements. A striking feature that Klatzo discovered was the presence of round and oval-shaped amyloid plaques with a diameter of 20-60 μm. These plaques were found in the granular layer of the cerebellum, basal ganglia, thalamus, and cerebral cortex. The neuropathology Igor Klatzo observed from kuru patients was reminiscent of Creutzfeldt-Jakob disease (CJD), which was described earlier by two German neurologists in the 1920s [14, 15]. The observed neuropathology puzzled Igor Klatzo. Therefore, he displayed the photos of the brain slices on in London in 1959 in hopes that someone would provide insight.

During the same time the photos were in London, William Hadlow, an American veterinarian, was sent to England by the NIH to learn more about scrapie due to an outbreak in the US during the late 1940s and early 1950s. Upon observation of the photos of the brain slices, Hadlow recognized a similar spongiform neuropathology between kuru and scrapie infected brains (Figure 3). In addition to the neuropathology, Hadlow noted that the ataxic symptoms and symptom duration found in kuru patients was also analogous to scrapie. He published these observations in the Lancet in 1959 [16]. Additionally, he proposed that kuru researchers attempt

transmission experiments using kuru-infected brains transmitted to laboratory primates.

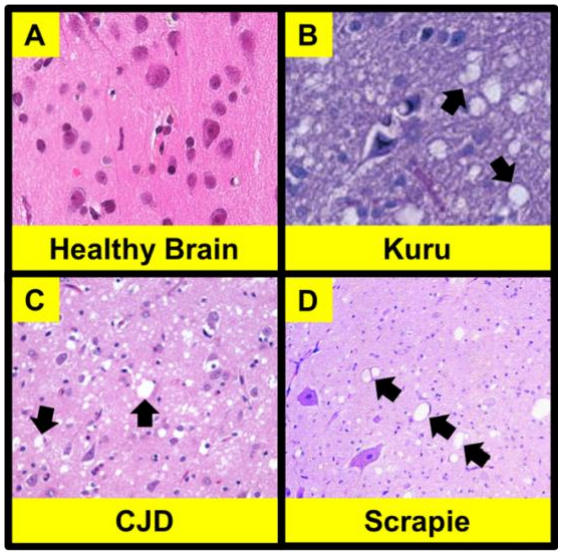

Figure 3: **Brain slices in different diseases.** Compared to the healthy brain (A) [17], the Kuru (B) [18], CJD (C) [19], and Scrapie (D) [20] brain slices have white holes (pointed at with black arrows) which is the characteristic spongiform found in these diseases.

In 1963, the first chimpanzee, a two-year-old female named Georgette, was intracerebrally inoculated with brain homogenate derived from a kuru patient [21]. Twenty months after the intracerebral injection, the chimpanzee began displaying signs of apathy and lack of energy. Eventually ataxic symptoms emerged and Georgette was unable to sit up and had difficulty feeding. Four months after symptom onset, Georgette was anesthetized and sacrificed. Neuropathological analysis revealed similar changes to Georgette's brain, such as spongiform in the cerebellum, when compared to kuru infected patients [22]. Overall, from the symptom and neuropathological similarities, Gajdusek concluded that kuru had been effectively transmitted [21].

Later in 1968, Clarence Gibbs successfully intracerebrally transmitted CJD-derived brain homogenate to a chimpanzee, which resulted in the chimpanzee displaying a similar disease progression and neuropathology as the CJD patient from which the material was derived from [23]. This led to the conclusion that the brain homogenate from the CJD patient contained a “transmissible agent” that initiated the disease in the chimpanzee. Ultimately, this conclusion suggested CJD, kuru, and scrapie were all transmissible, leading to a new class of diseases called transmissible spongiform encephalopathies (TSEs). Eventually, Gajdusek won the Nobel Prize in Physiology or Medicine in 1976 for his "discoveries concerning new mechanisms for the origin and dissemination of infectious diseases." [24]. Now, with two human diseases, kuru and CJD, being equated with scrapie, it led to researching the transmissibility of these diseases to other animals, with bovine in the United Kingdom having the spotlight.

Cows Going Wild in the UK

During the 1980s in the United Kingdom, a new disease was emerging in cattle. The disease typically afflicted dairy cows between the ages of two and eight years old. Symptoms first started with uncoordinated movement and weight loss. However, the defining symptom was a change in attitude and behavior, which manifested in aggressive cows. This led to colloquially calling the disease “Mad Cow Disease”. Neuropathological examination exhibited a clear resemblance to CJD, scrapie, and kuru infected brains [25]. Additionally, the deceased cows brains were ridden with

amyloid fibers [25], which at this point of time was considered an additional diagnostic for TSEs [26, 27]. Mad Cow Disease was officially termed Bovine Spongiform Encephalopathy (BSE) and added to the growing list of TSEs.

After a large population cattle succumbed to the disease, the Ministry of Agriculture, Fisheries, and Food (MAFF) decided it was time to determine the source of the disease. After the investigation, MAFF determined the commonality between the dying cows was that their diet contained meat and bone meal (MBM) [28]. Meat and bone meal is produced from the carcass and other body parts of animals, including sheep and cattle, that were deemed unfit for human consumption. Unfortunately, there almost certainly was a TSE-infected carcass, either sheep, bovine, or even human [29], that contaminated batches of MBM, eventually being fed to an enormous population of cattle distributed throughout the UK in the late 1970s and early 1980s [30, 31]. Due to the long incubation period, the disease was primarily observed in dairy cows, and not in beef cattle, owing to the fact that beef cattle are typically slaughtered by age two.

Once MAFF recognized contaminated MBM as a likely source of the BSE outbreak, the government banned these products from being fed to cattle in 1988. Eventually, in 1996, a ban was put in place to prevent feeding mammalian-derived MBM to any livestock, fish, or horses. Even with the implementation of these bans, many infected cow products were already in the human food supply. More

importantly, it was unknown if BSE-infected beef could transmit the disease to humans.

Between 1994 and 1996, 10 cases of CJD in the United Kingdom were reported to the CJD Surveillance Unit, with the first one being an 18-year-old named Stephen Churchill [32]. Once described as a happy and upbeat person, starting in October 1994, Stephen began isolating himself. By November 1994, his parents began noticing that Stephen was becoming more forgetful than normal. This soon became increasingly severe and he began to deteriorate mentally and started losing weight. Eventually in January 1995, his concerned parents decided to check him in to a psychiatric hospital. Once there, he started exhibiting neurological symptoms consisting of myoclonus and dysarthria. Doctors clearly recognized he did not have psychiatric problems, but rather neurological symptoms. After additional neurological tests, doctors told Stephen's parents that he had an incurable and progressive neurodegenerative disease. Finally on May 21st 1995, Stephen Churchill passed away from bronchopneumonia. The subsequent neuropathological evaluation revealed that his brain contained spongiform and astrocytosis. Doctors concluded the cause of death was CJD. This diagnosis was puzzling because CJD typically affected individuals in their 60s, but Stephen was under 30 years old.

Shortly after Stephen's death, more people under the age of 30 were dying of CJD (Figure 4). There was a clear neuropathology for all of these cases that resembled CJD; however, doctors also observed "florid" plaques around the spongiform in the

brain, particularly in the cerebellum, which is not common in classic CJD [33]. Additionally, the disease that affected Stephen Churchill and the others initially manifested itself with psychiatric symptoms, progressed more slowly than classic CJD, and affected younger people [34]. After serious deliberation, the United Kingdom's Department of Health announced on March 20, 1996 that these deaths were linked to BSE. Thus, this new TSE was named variant CJD (vCJD), and was determined to be contracted by ingesting BSE-contaminated beef. Now determining the identity of the toxic species became a very important question that scientists had to start answering.

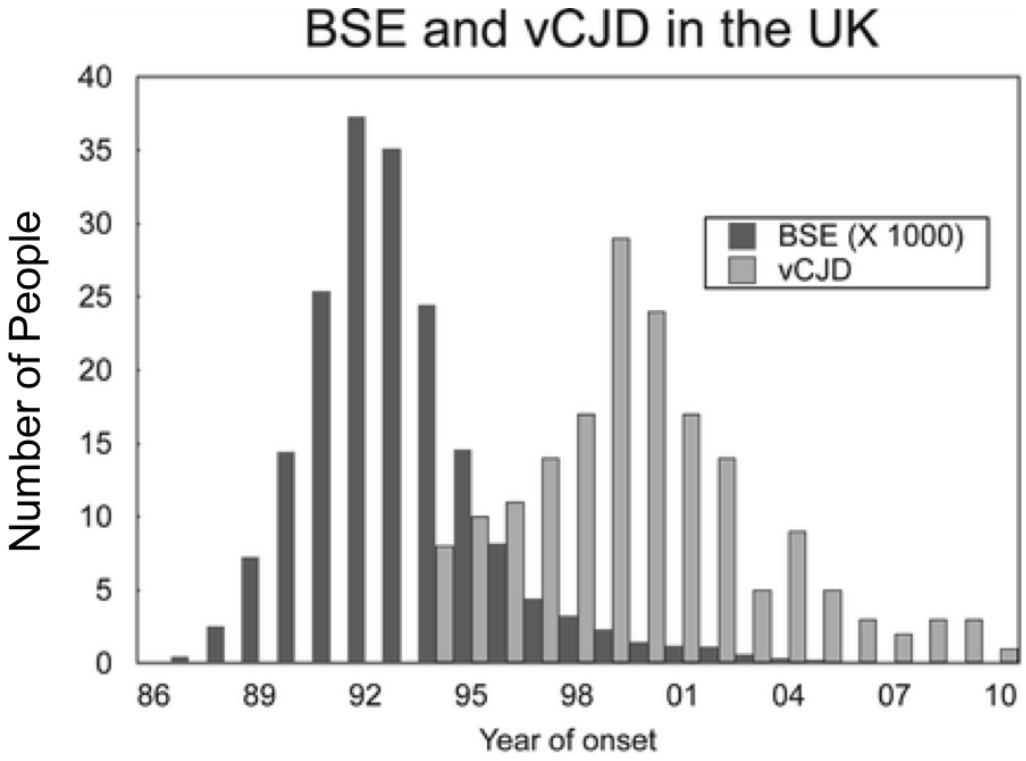

Figure 4: **Time line of BSE epidemic as compared to vCJD cases from 1986 to 2010 [35].** The peak of the BSE epidemic was in 1992. In contrast, the peak of the vCJD cases was 1999. This clearly shows the incubation period from the time of ingesting the infected beef to the year of symptom onset.

The Discovery of a New Infectious Biological Agent

In the 1960s, scientists began asking from what organism the toxin originated. Up until this time, infectious diseases, in accordance with Koch's postulates, were understood to be contracted by parasites, bacterial infections, funguses, or viruses. Koch's postulates states that the infectious microorganism must be able to be isolated from the sick and propagated in pure culture. This newly cultured microorganism should then be able to infect a new healthy organism with the same disease and subsequently be able to be reisolated. These were classically believed to be nucleic acid-containing microorganisms and upon infection would normally cause an immune response such as swelling, fever, or chills. Therefore, for these historical reasons, TSEs were then considered to be a "slow virus" [6, 36].

However, the infectious agent in TSEs displayed some peculiarities that made it seem unique and distinct from classical nucleic acid containing pathogens. The first clue came from how the looping ill virus vaccine was prepared [7]. The scrapie-infected looping ill virus vaccine was treated with 0.35% formalin, which would attenuate a virus or bacteria. However, the supposedly attenuated vaccine still resulted in sheep developing scrapie. Furthermore, in 1965, Iain Pattison treated infected scrapie brains with up to 20% formalin and still observed infectivity [37]. This led Pattison to propose that the infectious material may be protein in origin.

The second clue that the toxic species was not a classic pathogen came from Gajdusek and Gibbs. They would filter infectious brain homogenate through a 0.22

μm filter for their transmission experiments. This treatment filters out bacteria and larger particles [38]. Nonetheless, the homogenate remained infectious. However, this did not rule out the pathogen to be a virus, which could be anywhere from 0.017 to 0.3 μm and even larger [39].

The major clues that the pathogen was not a virus, or nucleic acid in nature, came from the British scientist Tikvah Alper. Using high energy electron bombardment experiments, Alper revealed the infectious particle was about 10 times smaller than any known virus [40]. Furthermore, Alper then demonstrated that the infectivity of the pathogen is not reduced upon irradiation with UV light (254 nm) that breaks down DNA and essentially deactivates viruses [41]. In contrast, and most importantly, the infectivity was slightly reduced when irradiated with UV light (280 nm) that would inactivate proteins. Overall, it appeared that these TSEs might be caused by something other than a virus or bacteria.

The results discussed above suggest that TSEs are most likely not caused by a nucleic acid containing pathogen. This led the biophysicist J.S. Griffiths to propose an interesting, but controversial, pathogenic mechanism as the basis for TSEs. Griffiths suggested a model based upon theoretically-driven arguments in which a misfolded form of a protein could potentially cause the normal folded form of a protein to convert into the misfolded form by template-driven misfolding (Griffiths 1967). This implied that the misfolded form can propagate and potentially lead to pathogenesis. This new type of model for disease pathogenesis led Griffiths to say “there is no

reason to fear that the existence of a protein agent would cause the whole theoretical structure of molecular biology to come tumbling down." [42]. What Griffiths meant was that just because this infectious and transmissible disease could be theoretically initiated by a protein misfolding event, does not mean the central dogma of molecular biology is incorrect, but rather different paradigms of diseases are able to exist. What Griffiths did not know was that he was on to something that would challenge the way scientist and doctors thought of infectious diseases.

The New Player on the Block

In 1972, Stanley Prusiner, a young medical resident at the University of California San Francisco, received a patient whose symptoms were consistent with CJD. He began pouring through the literature and found CJD and TSEs in general a very peculiar set of diseases. He was quite skeptical of the "slow virus" hypothesis [36]. His curiosity and skepticism were the catalysts for him to embark on the journey of discovering the identity of the scrapie agent. Therefore, he teamed up with William Hadlow and Carl Eklund at the Rocky Mountain Laboratory with the goal of purifying out the toxic scrapie agent. In 1978 after doing a countless number of end point titrations and going through over 10,000 mice, Prusiner realized something had to change to increase throughput. Thus, he modified how they were doing end point titrations as well as switched from using mice to using Syrian Hamsters [43]. This latter

change was of significance because Syrian Hamsters succumbed to TSEs twice as fast as mice [44], which significantly increased throughput.

Over the next couple of years, Prusiner and his team were able to purify samples that retained equivalent toxicity as crude brain homogenate [45], except the purified material was composed primarily of the scrapie agent. Furthermore, biochemical experiments demonstrated that the infectious species ranged in size from smaller than the smallest virus [46] to the size of a mitochondria or a bacterium [47]. Interestingly, all of the different sized particles were infectious. Consistent with previous studies, Prusiner found the particles were still infectious when exposed to nucleases, and in contrast lost infectivity when exposed to protein denaturants [48]. Furthermore, when the infectious particles were passed through different sized filters, Prusiner measured the size of the smallest toxic particle to be a mass of 50-100 kDa [45], or 5 nm in size, which is 1/100 the size of the smallest known virus. If the infectious agent was nucleic acid in origin, the length of the sequence would be limited to about 50 nucleotides, which is far too small for any known virus. However, if it was a protein, it would contain roughly 250 amino acids, which is a reasonable size for a protein. Overall, this mountain of evidence kept leading Prusiner down the path of reasoning that the infectious particle must be composed of a protein and not nucleic acids.

In 1982, Prusiner published a landmark paper in *Science* wherein he referred to the toxic particle as a protein and called it a ‘prion’ for it being a proteinaceous

particle [45]. In the highly pure and infectious material, Prusiner was able to find amyloid-like fibers that showed birefringence when stained with Congo red dye, indicative of a protein species [49]. Next, using classical peptide sequencing techniques, Prusiner, with the help of Leroy Hood and Charles Weissman, was able to identify the N-terminal peptide sequence of the prion protein [50]. Subsequently using DNA probes [51], they determined that the DNA coding for this peptide sequence was not only present in sick patients, but also in healthy tissues [52, 53] with high expression levels in the brain and heart.

With it now deduced that the infectious particle is protein in nature, Prusiner used proteinase K, a powerful protease, and determined that there are two forms of the protein due to the differential susceptibility to proteolysis [51]. He denoted the one form the cellular prion protein (PrP^{C}), which was found in healthy tissues and is fully degrade by proteinase K. In contrast, the second form of the same protein found in TSE infected brains is only partially degraded by proteinase K and is denoted as the scrapie form of the prion protein (PrP^{Sc}). Therefore, he concluded that there are two chemically identical proteins, but their three dimensional folds must be different to allow for PrP^{Sc} to be only partially degraded by proteinase K. Overall, Prusiner was able to bring it back full circle to the hypothesis laid forward by J.S. Griffiths in the 1960s, in which TSEs could be caused by a protein misfolding event.

If the prion model is valid, in which a protein misfolding event is at the core of TSEs, the hypothesis had to be rigorously tested. When the normal host prion protein

expression level was modulated in transgenic mice, the animals with higher PrP^{C} expression in the brain succumbed to the disease more rapidly [54]. Additionally, when PrP^{C} knockout mice (PrP) [55] were challenged with PrP^{Sc}, the mice did not succumb to the disease, nor did they produce any detectable amounts of PrP^{Sc} [56-58]. Furthermore, when $PrP^{-/-}$ mice containing a brain graft from a WT mouse were challenged with PrP^{Sc}, there was only PrP^{Sc} production in the brain graft, which spread throughout the brain of the $PrP^{-/-}$ mice [59]. Importantly, the $PrP^{-/-}$ mice containing the brain graft survived and there was no measurable toxicity [59]. Overall, these studies elucidated that the normal host prion protein is required for the neurotoxicity induced by PrP^{Sc} and the expression level of PrP^{C} is correlated with disease progression.

However, these results could correlate with the hypothesis laid out by Griffiths in 1967, where PrP^{Sc} would directly interact with PrP^{C} to cause its misfolding. Conversely, infecting animals with PrP^{Sc} could cause PrP^{C} to become misfolded by indirect interactions. To test this hypothesis, Prusiner developed transgenic mice to express both Syrian hamster PrP^{C} ($SHaPrP^{C}$) and mouse PrP^{C} ($MoPrP^{C}$) [54]. Using different antibodies that can selectively differentiate $SHaPrP^{Sc}$ and $MoPrP^{Sc}$, it was determined that when the animals were exposed to hamster-derived PrP^{Sc}, the mouse selectively produced $SHaPrP^{Sc}$ and not $MoPrP^{Sc}$. Conversely, when the mice were challenged with $MoPrP^{Sc}$, the mice produced only $MoPrP^{Sc}$. Overall, this study demonstrated multiple findings. First, PrP^{Sc} directly interacts with the infected hosts

PrP^C. Secondly, these results implicate a species barrier between the origin of the PrP^{Sc} and the species of the infected animal. This means that the information encoded in the misfolded protein originates from its amino acid sequence, which in turn dictates the three-dimensional structure or the misfolded PrP^{Sc}. This will subsequently enable the protein to directly dock to the hosts PrP^C with sequence specificity, and if the interaction is correct, it will induce misfolding of the host's PrP^C into PrP^{Sc}. Therefore, due to the amino acid sequence differences between $SHaPrP^C$ and $MoPrP^C$, when a mouse expressing both proteins is challenged with mouse-derived PrP^{Sc}, $MoPrP^C$ will selectively dock to the $MoPrP^{Sc}$.

From this logic, the misfolded forms originating from different species are considered to be a particular strain, and these different strains can have different three-dimensional structures. Additionally, it has been known since the late 1980s that familial mutations in the prion protein gene can elicit a predisposition to prion diseases [60, 61]. These human prion diseases include CJD, Gerstmann–Sträussler–Scheinker syndrome (GSS), and Fatal Familial Insomnia (FFI). Even though these diseases all result in the misfolding of PrP^C, they have different incubation periods, different symptoms and symptom durations, different affected brain regions, and different strains. The different strains can be differentiated by proteinase K digestion and followed by western blotting. For example, proteinase K digestion of PrP^{Sc} derived from patients with FFI results in a protease resistant fragment with an apparent molecular weight of 19 kDa [62]. In contrast, proteinase K digested PrP^{Sc} derived from

CJD patients containing the E200K mutation results in a protease resistant fragment with an apparent molecular weight of 21 kDa [62]. Furthermore, when a transgenic mouse expressing a chimeric mouse and human prion protein (Tg(MHu2M) mice) (Telling 1994) was inoculated with PrP^{Sc} derived from a patient with FFI, the mouse produced the 19 kDa protease resistant fragment [63]. Conversely, when the Tg(MHu2M) mice was inoculated with CJD patient derived PrP^{Sc}, the mice produced the 21 kDa protease resistant fragment. Additionally, the distribution of PrP^{Sc} in the brains of the infected Tg(MHu2M) was different depending on which strain was inoculated. Overall, these results demonstrate that the strain encodes the information of not only how the host's PrP^{C} is going to misfold, but also what brain region gets affected and what the symptoms will be.

So what does the scientific community know at this point? It is known that TSEs affecting humans and other mammals are all caused by the misfolding of the hosts PrP^{C} to generate the aggregation prone PrP^{Sc} conformer. We also know that these diseases are transmissible and infectious. However, there is a species barrier in which the amino acid sequence of the protein dictates its structure, which consequently determines how efficiently it can misfold the hosts PrP^{C}. This is likely the reason why mad cow disease only killed around 200 people [64] when a large population consumed tainted beef. We also know that these diseases can be initiated by familial mutations in the host's prion protein gene. Additionally, CJD can arise

spontaneously without the need for a pathological mutation, which accounts for around 85% of the diagnosed cases [65].

From many years of research, the prion model of infection has been proposed (Figure 5). It is initiated by either ingesting PrP^{Sc} or having a spontaneous or familial mutation driven misfolding event of PrP^{C} into an aggregated PrP^{Sc} seed. Once this PrP^{Sc} seed occurs, it subsequently docks to the hosts PrP^{C}, causing it to become misfolded. Furthermore, the buildup of PrP^{Sc} results in larger aggregates, which eventually shears into smaller aggregates. In turn, these smaller aggregates spread throughout the brain, resulting in producing more PrP^{Sc} aggregates. Eventually, this leads to downstream events that generates astrocytosis and massive neurodegeneration. The region of this neurodegeneration will determine the symptoms. Ultimately, the extensive neurodegeneration will result in the patient or animal to succumb to death.

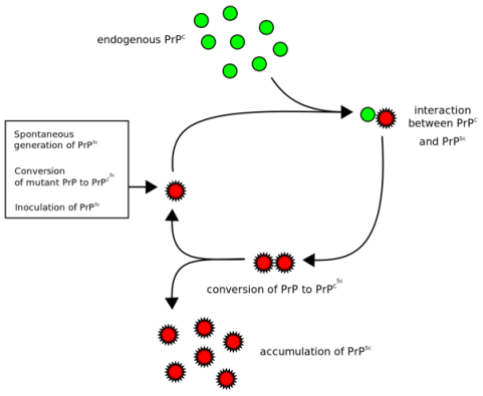

Figure 5: **Prion propagation mechanism.** First there is a PrP^{Sc} seed by either spontaneous misfolding, by inoculation with PrP^{Sc}, or conversion of PrP^{C} to PrP^{Sc} by familial mutation. This misfolded form will bind to endogenous PrP^{C} and converting it to PrP^{Sc}. Eventually you accumulate PrP^{Sc} and toxicity occurs [66].

Unfortunately, there is no cure for TSEs and the toxic mechanisms behind the neurotoxicity is not completely understood. To gain a better understanding of the neurotoxicity elicited by TSEs with the goal of developing therapeutics, it is critical to understand the biology of native PrP^C. Additionally, it is important to decipher the native function and structure of PrP^C to achieve a better understanding of how the system can fail during TSEs and elicit neurotoxicity.

Biology of The Cellular Prion Protein

The human prion protein gene (Prnp) is encoded on chromosome 20 [67]. PrP^C is expressed throughout the body; however, it is highly enriched in the brain and neurons [68-70]. The protein is initially expressed as a 254 amino acid pro-protein. The 22 N-terminal amino acids contain a signal peptide sequence that allows for translocation to the endoplasmic reticulum. Subsequent to translocation, the 22 N-terminal amino acids are removed by proteolysis. Additionally, the 23 C-terminal amino acids are removed after the addition of a glycophosphatidylinositol (GPI) anchor to yield a mature 208 amino acid protein, PrP(23-230). During transit through the Golgi apparatus, N-linked glycans are variably added to Asn180 and Asn197 to produce either an un-, mono-, or diglycosylated glycoprotein. Lastly, a disulfide bond is formed between Cys178 and Cys214, which helps maintains a rigid structure. Once the fully matured PrP^C passes through the Golgi apparatus, PrP^C is trafficked to the

cell surface. The GPI anchor on the C-terminus keeps PrP^C membrane-associated, where it is found in cholesterol-rich microdomains called lipid rafts [71].

Initial structural studies revealed that PrP^C is primarily α-helical and PrP^{Sc} is predominantly composed of ß-sheets [72]. Later, using nuclear magnetic resonance (NMR), Kurt Wüthrich's group revealed PrP^C is composed of two major domains: an unstructured N-terminal domain (23-125) and a structured C-terminal domain (Figure 6) [73-75]. Eventually, Wüthrich's group used NMR to elucidate the high resolution three dimensional structure of the C-terminal domain of PrP^C [75]. They determined the C-terminal domain of PrP^C is composed of three α-helices, one short anti-parallel ß-sheet, and one disulfide bond (Figure 6).

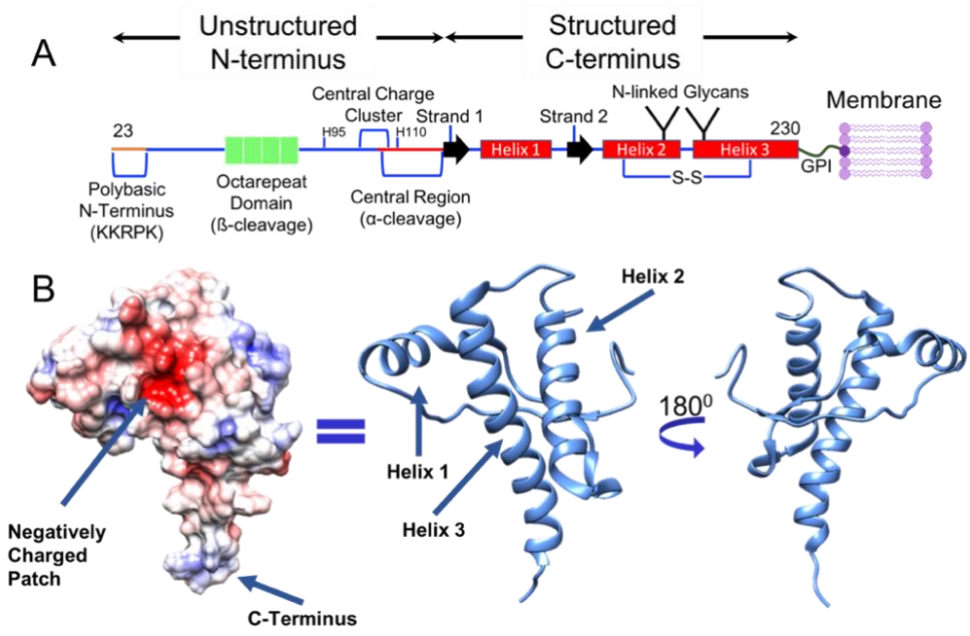

Figure 6: **Schematic and structure of PrP^C.** (A) Linear schematic of PrP^C and the different domains. (B) To the left is the electrostatic potential map of the C-terminus (amino acids 125-230) which shows a negatively charged patch in red. The middle and right figures are ribbon structures determined by NMR structure determination of the C-terminus which shows three α-helices and one antiparallel sheet. (PDB: 1XYX).

In contrast to the C-terminal domain, the N-terminal domain is completely unstructured. Nevertheless, it is rich in functionality and contains two major motifs. The first motif is the polybasic N-terminus (residues 23-31), which is rich in basic amino acids and is implicated in interacting with membrane receptors such as the AMPA receptor (AMPAR) [76]. The polybasic N-terminus is also capable of binding to PrP^{Sc} and aiding in the efficient template driven misfolding event [77]. Transgenic mice expressing a mutant PrP^{C} in which the polybasic N-terminus is deleted (Tg(Δ23-31)) show a reduced susceptibility to PrP^{Sc} infection in addition to a drastic reduction in PrP^{Sc} production [77]. The second major motif in the unstructured N-terminus is the octarepeat (OR) domain (residues 59-90). The OR is composed of four repeats of eight amino acids (PHGGGWGQ) [78] that are able to bind up to four copper (Cu^{2+}) ions or one zinc (Zn^{2+}) ion at physiological concentrations and pH [78-82]. It has been previously shown that Cu^{2+} binding to the OR is pH and Cu^{2+} concentration dependent [78]. At neutral pH, the OR can bind to Cu^{2+} using two main binding modes (Figure 7). At low Cu^{2+} concentrations, Cu^{2+} will bind to one histidine residue contained in each repeat with a square planar geometry. This binding mode is called component 3 and has an affinity of 0.12 nM [83]. At higher Cu^{2+} concentrations, each repeat will bind one Cu^{2+} ion using the minimum binding motif of HGGGW [80]. This binding mode is called component 1 and has an affinity of 7-12 μM [83]. Therefore, depending on the Cu^{2+} concentration, the OR of PrP^{C} can act as a Cu^{2+} buffer because it possesses the ability to coordinate between one and four Cu^{2+} ions.

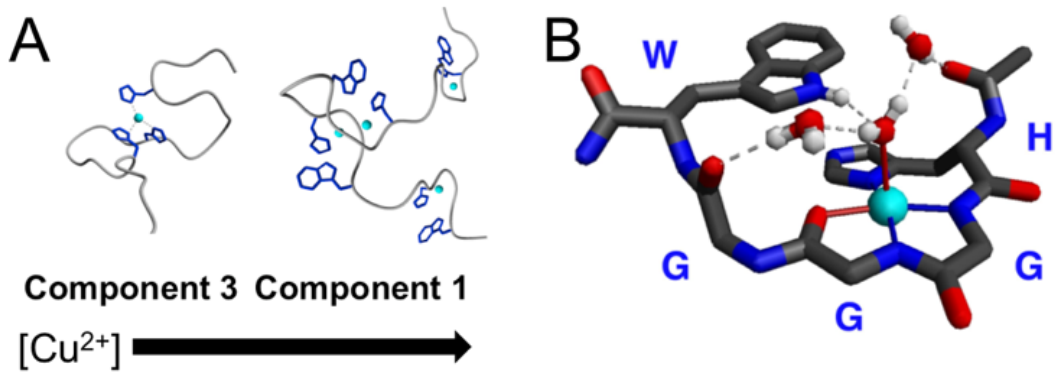

Figure 7: **Different binding modes of Cu^2 to the OR of PrP^C [78]. A.** At low Cu^{2+} conditions, the OR can bind to one Cu^{2+}. At higher Cu^{2+} conditions, the OR can bind up to four Cu^{2+} ions using the minimum binding motif of HGGGW **(B)**.

The ability of PrP^C to bind to metal ions has implicated metal binding as an integral part of PrP^C function. It has been demonstrated that Cu^{2+} increases PrP^C expression levels [84]. Additionally, early studies have shown that $PrP^{-/-}$ mice display a decreased neuronal membrane Cu^{2+} concentration [85]. Moreover, Pushie and colleagues determined that the distribution of Cu^{2+}, Zn^{2+}, and Fe^{2+} ions are all altered in $PrP^{-/-}$ mice when compared to wild-type mice or mice over expressing PrP^C [86]. Evolutionarily, PrP^C is related to the ZIP family of metal ion transporters [87]. In cell culture, Cu^{2+} [88, 89] and Zn^{2+} [90] stimulate PrP^C endocytosis using low-density lipoprotein receptor-related protein 1 (LRP1) as a co-receptor [88, 89]. This metal-driven endocytosis is reduced in familial mutations in the OR that drive prion diseases [90]. Additionally, Zn^{2+} binding to the OR aids in AMPAR uptake of Zn^{2+} ions [76, 91]. Overall, metal binding to PrP^C is intimately tied to PrP^C function.

It was once thought that the unstructured N-terminus and the structured C-terminus act independently. However, recent NMR and electron paramagnetic resonance (EPR) experiments demonstrate that they do interact in a Cu^{2+} or Zn^{2+} dependent manner [92-97]. This interaction, termed the metal-driven *cis*-interaction, occurs when one Zn^{2+} [95] or Cu^{2+} [92, 94] ion binds to the OR (Figure 8). This drives an interaction between the metal-bound OR and a conserved negatively charged patch on the C-terminus [94, 98, 99].

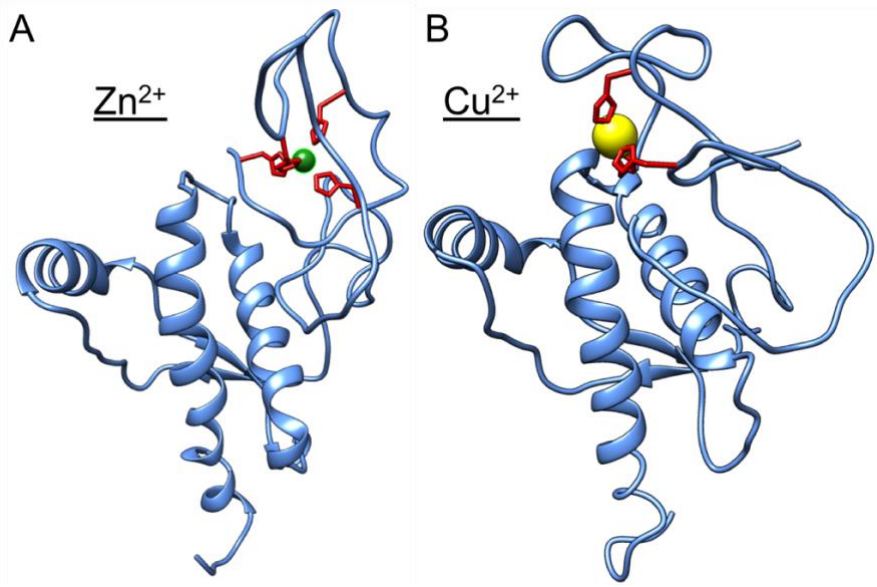

Figure 8: **Models of the metal-driven *cis*-interaction.** A model of PrP^C binding to a Zn^{2+} ion (A) or Cu^{2+} ion (B) with OR histidine residues [92, 95]. The binding of these ions drives the interaction between the unstructured N-terminus and the structured C-terminus.

The metal-driven *cis*-interaction is of relevance due to recent experiments demonstrating C-terminal-directed antibodies, whose epitope overlaps with where the metal-bound OR docks to the C-terminus when engaged in the metal-driven *cis*-interaction [92], trigger neurotoxicity in animals and cell models [100]. The cellular

response elicited by C-terminal antibodies is similar to that found in natural prion diseases, such as generation of reactive oxygen species (ROS), stimulation of the unfolded protein response, and down-regulation of similar genes [101]. Additionally, antibodies targeting the N-terminus are able to block C-terminal antibody-induced neurotoxicity [100] as well as reduce PrP^{Sc} toxicity [101]. This suggest a model in which the N-terminus has an effector function with toxic potential that is regulated by the C-terminus via the *cis*-interaction. It is hypothesized that if the *cis*-interaction is blocked, toxicity is induced via the N-terminal toxicity model [102] (Figure 9). Interestingly, a number of familial mutations on the C-terminus change the charge from negative to neutral or negative to positive, and these mutations have been previously shown to weaken the metal-driven *cis*-interaction [94, 95, 98], which further supports the hypothesis that the toxic potential of the N-terminus is regulated by the C-terminus.

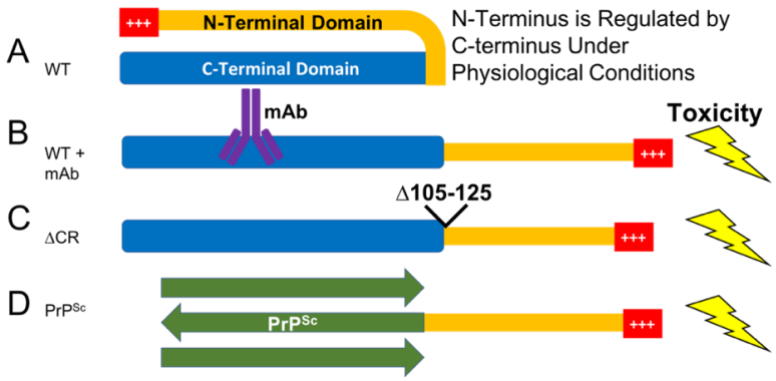

Figure 9: **N-terminal toxicity model.** The N-terminus of WT PrP^{C} (A) is regulated by the C-terminus under physiological conditions, presumably through the metal-driven *cis*-interaction and no toxicity occurs. However, when C-terminal monoclonal antibodies (mAb) bind to WT PrP^{C} (B) or by deletion of residues 105-125 (ΔCR PrP^{C}), toxicity occurs. Additionally, it is hypothesized that the C-terminus of PrP^{Sc} (D) is unable to regulate the unstructured N-terminus. The N-terminal toxicity model is dependent on the presence of the polybasic N-terminus (red).

One of the most highly-conserved regions of the prion protein throughout species is the intervening segment between the N- and C-terminal domains called the central region (CR: residues 105-125) [103, 104]. Notably, the CR undergoes a regulatory cleavage event termed α-cleavage [105-107] to produce a membrane-bound C-terminal fragment (C1) and a released N-terminal fragment (N1). The N1 fragment binds and agonizes Adgrg6, a G protein-coupled receptor (GPCR) that regulates myelination in Schwann cells [108]. Additionally, the C1 fragment has been shown to act as a dominant negative inhibitor of PrP^{Sc} formation because it can bind to PrP^{Sc} aggregates, but does not get converted into PrP^{Sc} [109]. There is an additional cleavage event that occurs in the OR called ß-cleavage. In contrast to α-cleavage, ß-cleavage only occurs to a small degree in healthy tissues. However it is upregulated in prion diseases, perhaps for antioxidant purposes [110] and produced by an ROS mechanism [111].

Central Region Deletion Mutants as a Model System for Prion Diseases

Prion diseases are known to have a slow progression. Unfortunately, even with overexpression systems in mice, which are designed to speed up the disease progression [112], prion research can still be slow. Therefore, it is important to have suitable model system to accelerate the research process. This was aided by studies investigating deletion mutants within the unstructured N-terminus. When trying to discover which domains are important for function, researchers remove portions of

the protein to observe the resulting phenotype. In 1998, Doron Shmerling and coworkers generated the deletion mutant ΔF PrP^{C} (Δ32-134) that resulted in mice displaying ataxia and cerebellar lesions [113]. The phenotype is also reversible upon expression of one copy of WT PrP^{C}. Eventually, these mice die two to three months after birth. The mice efficiently expressed ΔF PrP^{C} on the cell surface, however there was no measurable PrP^{Sc} production. Therefore, this suggested that the neurodegeneration observed mimicked PrP^{Sc}, except death was accelerated because there was not a need for the slow buildup of PrP^{Sc}.

Further investigation into amino-terminal proximal deletions revealed that the shorter the deletion, the more rapidly the mice would perish. However, it was recognized that the deletion must encompass the CR of PrP^{C} and still retain the polybasic N-terminus. Furthermore, deletion of residues 94-134 (ΔCD PrP^{C}) resulted in dramatic neurodegeneration and death in the mice between 20 and 30 days [114]. Additionally, ΔCD mice have a demyelinating polyneuropathy phenotype that is also seen in $PrP^{-/-}$ mice [115] and CJD patients [116, 117]. Remarkably, the shortest deletion of just the central region (Δ105-125: ΔCR PrP^{C}) resulted in the most drastic neurodegenerative phenotype in mice and neonatal fatality around one week after birth [118, 119].

Due to the drastic phenotype of ΔCR PrP^{C} mice, it has been extensively investigated [94, 97, 118, 120-125]. In cell culture and transgenic mice, ΔCR PrP^{C} is trafficked and post-translationally modified identical to WT PrP^{C} [118]. Additionally,

ΔCR PrP^C displays spontaneous currents in whole cell patch clamp electrophysiological measurements in cell culture and primary neurons [121, 126]. Additionally, ΔCR PrP^C expressing cells are show a decrease in cell viability when treated with cationic antibiotics [127]. Furthermore, ΔCR PrP^C sensitizes cells to glutamate-induced excitotoxicity [121], which is also observed in bona fide prion infection [128]. Overall, these results suggest that ΔCR PrP^C causes an unregulated flow of ions or charged species across the membrane, either by membrane destabilization [129], or by over-activation of membrane ion channels.

The spontaneous current phenotype found in ΔCR PrP^C is also observed when WT PrP^C expressing cells are treated with C-terminal antibodies [97]. This observation is reversed with co-administration of N-terminal antibodies [97]. This result parallels C-terminal antibody-induced toxicity [100]. Furthermore, deletion of the polybasic N-terminus renders ΔCR PrP^C and C-terminal antibody-induced neurodegeneration non-toxic, suggesting the polybasic N-terminus has toxic potential. Moreover, it was shown that ΔCR PrP^C has a weakened Cu^{2+}-driven *cis*-interaction [97]. Overall, these results suggest that the CR, in addition to the C-terminus, of PrP^C has a protective role over the intrinsic toxic potential of the N-terminus. Understanding how the CR regulates the toxic potential of the N-terminus is important to better understand the toxic mechanism of PrP^{Sc}.

Specific Aims

It is known that PrP^C deletions encompassing the CR cause extensive neurodegeneration paralleling PrP^{Sc} induced neurotoxicity. However, it is unknown what change is occurring in ΔCR PrP^C that is driving the toxicity. It is observed that ΔCR PrP^C displays a weakened Cu^{2+}-driven *cis*-interaction [97]. Blocking this regulatory interaction would allow for the release of the toxic N-terminus from the regulatory C-terminus. Moreover, according to the N-terminal toxicity model, this could lead to membrane destabilization or glutamate receptor over-activation [102], and thus neurotoxicity. Alternatively, the CR contains the regulatory α-cleavage site, thus ΔCR PrP^C does not undergo α-cleavage to generate the biologically active N1 fragment. Furthermore, α-cleavage not only produces the biologically active N1 fragment, but it also gives a pathway to deactivate PrP^C from regulating its binding partners [107].

This means that ΔCR PrP^C has two major changes that could lead to toxicity: 1) weakening of the metal-driven *cis*-interaction, and 2) deletion of the locus for α-cleavage. Therefore, the first specific aim of this dissertation is to determine if weakening the *cis*-interaction or blocking alpha cleavage or potentially something else is driving ΔCR PrP^C induced toxicity. This was accomplished by designing PrP^C constructs that allow for one of these changes (blocked metal-driven *cis*-interaction or blocked α-cleavage) at a time while simultaneously retaining the other. These

designed constructs were then assessed using NMR, *in vitro* and cellular cleavages assays, electrophysiology, and cell based viability assays.

a *cis*-interaction is general to all familial prion diseases, or if it is mutually exclusive to C-terminal familial mutations.

In summary, the specific aims of this dissertation are:

1. To determine if weakening the Cu^{2+}-driven *cis*-interaction or blocking α-cleavage or something else drives ΔCR PrP^C induced toxicity.
2. To determine if weakening of the Cu^{2+}-driven *cis*-interaction of PrP^C can be attributed to all familial mutations that drive prion diseases, or if it only occurs in C-terminal mutations.

References

1. Brown, P. and R. Bradley, *1755 and all that: a historical primer of transmissible spongiform encephalopathy.* BMJ, 1998. **317**(7174): p. 1688-92.
2. West, D.M., et al., *The sheep : health, disease and production*. Fourth revised edition. ed. 407 pages.
3. Commons, H.o., *Journals of the House of Commons*. 2015, TannerRitchie Publishing,: S.l.
4. Besnoit C, M.C., *Note sur les lésions nerveuses de la tremblante du mouton.* Rev Vet, 1898. **23**(Le): p. 397-400.
5. Besnoit, *La tremblante ou névrite périphérique enzootique du mouton.* Rev Vet, 1899. **23**: p. 307-343.
6. Cuillé J, C.P.L., *La maladie dite "tremblante" du mouton; est-elle inoculable?* Compte Rend Acad Sci, 1936. **203**: p. 1552.

7. Gordon, W.S., *Advances in veterinary research.* Vet Rec, 1946. **58**(47): p. 516-25.

8. Lindenbaum, S., *Kuru Sorcery : Disease and Danger in the New Guinea Highlands*. 2015: Routledge.

9. Gajdusek, D.C. and V. Zigas, *Studies on kuru. I. The ethnologic setting of kuru.* Am J Trop Med Hyg, 1961. **10**: p. 80-91.

10. Gajdusek, D.C. and V. Zigas, *Kuru; clinical, pathological and epidemiological study of an acute progressive degenerative disease of the central nervous system among natives of the Eastern Highlands of New Guinea.* Am J Med, 1959. **26**(3): p. 442-69.

11. Liberski, P.P., *Kuru: a journey back in time from papua new Guinea to the neanderthals' extinction.* Pathogens, 2013. **2**(3): p. 472-505.

12. Klitzman, R.L., M.P. Alpers, and D.C. Gadjdusek, *The Natural Incubation Period of Kuru and the Episodes of Transmission in Three Clusters of Patients.* Neuroepidemiology, 1984. **3**(1): p. 3-20.

13. Klatzo, I., D.C. Gajdusek, and V. Zigas, *Pathology of Kuru.* Lab Invest, 1959. **8**(4): p. 799-847.

14. Creutzfeldt, H.G., *Über eine eigenartige herdförmige erkrankung des zentralnervensystems* Zeitschrift für die gesamte Neurologie und Psychiatrie, 1920. **57**(1): p. 1-18.

15. Jakob, A., *Über eigenartige erkrankungen des zentralnervensystems mit bemerkenswertem anatomischen befunde.* Zeitschrift für die gesamte Neurologie und Psychiatrie, 1921. **64**(1): p. 147-228.

16. Hadlow, W.J., *Scrapie and Kuru.* Lancet, 1959. **2**(Sep5): p. 289-290.

17. Gordon, Z. *Prions — the Revenge of the Cows*. 2018; Available from: https://www.zmescience.com/medicine/prions-the-charismatic-proteins/.

18. Liberski, P.P., et al., *Kuru: genes, cannibals and neuropathology.* J Neuropathol Exp Neurol, 2012. **71**(2): p. 92-103.

19. Walker, L.C. and M. Jucker. *The Malignant Protein Puzzle*. 2016; Available from: https://www.dana.org/article/the-malignant-protein-puzzle/

.

20. Hamir, A.N., et al., *Experimental transmission of scrapie agent to susceptible sheep by intralingual or intracerebral inoculation.* Can J Vet Res, 2008. **72**(1): p. 63-7.

21. Gajdusek, D.C., C.J. Gibbs, and M. Alpers, *Experimental Transmission of a Kuru-Like Syndrome to Chimpanzees.* Nature, 1966. **209**(5025): p. 794-&.

22. Beck, E., et al., *Experimental Kuru in Chimpanzees - a Pathological Report.* Lancet, 1966. **2**(7472): p. 1056-&.

23. Gibbs, C.J., Jr., et al., *Creutzfeldt-Jakob disease (spongiform encephalopathy): transmission to the chimpanzee.* Science, 1968. **161**(3839): p. 388-9.

24. *The Nobel Prize in Physiology or Medicine 1976*. 1976.

25. Wells, G.A., et al., *A novel progressive spongiform encephalopathy in cattle.* Vet Rec, 1987. **121**(18): p. 419-20.

26. Merz, P.A., et al., *Infection-specific particle from the unconventional slow virus diseases.* Science, 1984. **225**(4660): p. 437-40.

27. Merz, P.A., et al., *Abnormal fibrils from scrapie-infected brain.* Acta Neuropathol, 1981. **54**(1): p. 63-74.

28. Wilesmith, J.W., et al., *Bovine spongiform encephalopathy: epidemiological studies.* Vet Rec, 1988. **123**(25): p. 638-44.

29. Colchester, A.C. and N.T. Colchester, *The origin of bovine spongiform encephalopathy: the human prion disease hypothesis.* Lancet, 2005. **366**(9488): p. 856-61.

30. Bradley, R., *Bovine Spongiform Encephalopathy Epidemiology - a Brief Review.* Livestock Production Science, 1994. **38**(1): p. 5-16.

31. Wilesmith, J.W., J.B. Ryan, and M.J. Atkinson, *Bovine spongiform encephalopathy: epidemiological studies on the origin.* Vet Rec, 1991. **128**(9): p. 199-203.

32. Yam, P., *The pathological protein : mad cow, chronic wasting, and other deadly prion diseases*. 2003, New York: Copernicus. xviii, 284 pages.

33. Will, R.G., et al., *A new variant of Creutzfeldt-Jakob disease in the UK.* Lancet, 1996. **347**(9006): p. 921-5.

34. McLean, C.A., *Review. The neuropathology of kuru and variant Creutzfeldt-Jakob disease.* Philos Trans R Soc Lond B Biol Sci, 2008. **363**(1510): p. 3685-7.

35. Brown, P., *Environmentally Acquired Transmissible Spongiform Encephalopathy*, in *Prions and Diseases: Volume 2, Animals, Humans and the Environment*, W.-Q. Zou and P. Gambetti, Editors. 2013, Springer New York: New York, NY. p. 73-88.

36. Sigurdsson, B., *RIDA, A Chronic Encephalitis of Sheep: With General Remarks on Infections Which Develop Slowly and Some of Their Special Characteristics.* British Veterinary Journal, 1954. **110**(9): p. 341-354.

37. Pattison, I.H., *Resistance of the Scrapie Agent to Formalin.* J Comp Pathol, 1965. **75**: p. 159-64.

38. Gajdusek, D.C., C.J. Gibbs, and M. Alpers, *Transmission and Passage of Experimental Kuru to Chimpanzees.* Science, 1967. **155**(3759): p. 212-&.

39. Gelderblom, H.R., *Structure and Classification of Viruses*, in *Medical Microbiology*, th and S. Baron, Editors. 1996: Galveston (TX).

40. Alper, T., D.A. Haig, and M.C. Clarke, *The exceptionally small size of the scrapie agent.* Biochem Biophys Res Commun, 1966. **22**(3): p. 278-84.

41. Alper, T., et al., *Does the agent of scrapie replicate without nucleic acid?* Nature, 1967. **214**(5090): p. 764-6.

42. Griffith, J.S., *Self-replication and scrapie.* Nature, 1967. **215**(5105): p. 1043-4.

43. Prusiner, S.B., et al., *Molecular properties, partial purification, and assay by incubation period measurements of the hamster scrapie agent.* Biochemistry, 1980. **19**(21): p. 4883-91.

44. Kimberlin, R.H. and R.F. Marsh, *Comparison of scrapie and transmissible mink encephalopathy in hamsters. I. Biochemical studies of brain during development of disease.* J Infect Dis, 1975. **131**(2): p. 97-103.

45. Prusiner, S.B., *Novel proteinaceous infectious particles cause scrapie.* Science, 1982. **216**(4542): p. 136-44.

46. Prusiner, S.B., et al., *Partial purification and evidence for multiple molecular forms of the scrapie agent.* Biochemistry, 1978. **17**(23): p. 4993-9.

47. Prusiner, S.B., et al., *Experimental scrapie in the mouse: electrophoretic and sedimentation properties of the partially purified agent.* J Neurochem, 1980. **35**(3): p. 574-82.

48. Prusiner, S.B., et al., *Thiocyanate and hydroxyl ions inactivate the scrapie agent.* Proc Natl Acad Sci U S A, 1981. **78**(7): p. 4606-10.

49. Prusiner, S.B., et al., *Scrapie prions aggregate to form amyloid-like birefringent rods.* Cell, 1983. **35**(2 Pt 1): p. 349-58.

50. Prusiner, S.B., et al., *Purification and structural studies of a major scrapie prion protein.* Cell, 1984. **38**(1): p. 127-34.

51. Oesch, B., et al., *A cellular gene encodes scrapie PrP 27-30 protein.* Cell, 1985. **40**(4): p. 735-46.

52. Chesebro, B., et al., *Identification of scrapie prion protein-specific mRNA in scrapie-infected and uninfected brain.* Nature, 1985. **315**(6017): p. 331-3.

53. Kretzschmar, H.A., et al., *Molecular cloning of a human prion protein cDNA.* DNA, 1986. **5**(4): p. 315-24.

54. Prusiner, S.B., et al., *Transgenetic studies implicate interactions between homologous PrP isoforms in scrapie prion replication.* Cell, 1990. **63**(4): p. 673-86.

55. Bueler, H., et al., *Normal development and behaviour of mice lacking the neuronal cell-surface PrP protein.* Nature, 1992. **356**(6370): p. 577-82.

56. Bueler, H., et al., *Mice devoid of PrP are resistant to scrapie.* Cell, 1993. **73**(7): p. 1339-47.

57. Prusiner, S.B., et al., *Ablation of the prion protein (PrP) gene in mice prevents scrapie and facilitates production of anti-PrP antibodies.* Proc Natl Acad Sci U S A, 1993. **90**(22): p. 10608-12.

58. Weissmann, C., et al., *PrP-deficient mice are resistant to scrapie.* Ann N Y Acad Sci, 1994. **724**: p. 235-40.

59. Brandner, S., et al., *Normal host prion protein necessary for scrapie-induced neurotoxicity.* Nature, 1996. **379**(6563): p. 339-43.

60. Aguzzi, A., F. Baumann, and J. Bremer, *The prion's elusive reason for being.* Annu Rev Neurosci, 2008. **31**: p. 439-77.

61. Prusiner, S.B., et al., *Prion protein biology.* Cell, 1998. **93**(3): p. 337-48.

62. Monari, L., et al., *Fatal familial insomnia and familial Creutzfeldt-Jakob disease: different prion proteins determined by a DNA polymorphism.* Proc Natl Acad Sci U S A, 1994. **91**(7): p. 2839-42.

63. Telling, G.C., et al., *Evidence for the conformation of the pathologic isoform of the prion protein enciphering and propagating prion diversity.* Science, 1996. **274**(5295): p. 2079-82.

64. *Facts about variant Creutzfeldt-Jakob disease*. 2017; Available from: https://www.ecdc.europa.eu/en/vcjd/facts.

65. Ladogana, A., et al., *Mortality from Creutzfeldt-Jakob disease and related disorders in Europe, Australia, and Canada.* Neurology, 2005. **64**(9): p. 1586-91.

66. tecywiz121. 2009; Available from: https://en.wikipedia.org/wiki/Prion#/media/File:Prion_propagation.svg.

67. Sparkes, R.S., et al., *Assignment of the human and mouse prion protein genes to homologous chromosomes.* Proc Natl Acad Sci U S A, 1986. **83**(19): p. 7358-62.

68. Barmada, S., et al., *GFP-tagged prion protein is correctly localized and functionally active in the brains of transgenic mice.* Neurobiol Dis, 2004. **16**(3): p. 527-37.

69. Peralta, O.A. and W.H. Eyestone, *Quantitative and qualitative analysis of cellular prion protein (PrP(C)) expression in bovine somatic tissues.* Prion, 2009. **3**(3): p. 161-70.

70. Sales, N., et al., *Cellular prion protein localization in rodent and primate brain.* Eur J Neurosci, 1998. **10**(7): p. 2464-71.

71. Watt, N.T., H.H. Griffiths, and N.M. Hooper, *Lipid rafts: linking prion protein to zinc transport and amyloid-beta toxicity in Alzheimer's disease.* Front Cell Dev Biol, 2014. **2**: p. 41.

72. Pan, K.M., et al., *Conversion of alpha-helices into beta-sheets features in the formation of the scrapie prion proteins.* Proc Natl Acad Sci U S A, 1993. **90**(23): p. 10962-6.

73. Hornemann, S., et al., *Recombinant full-length murine prion protein, m PrP(23-231): purification and spectroscopic characterization.* FEBS Letters, 1997. **413**(2): p. 277-281.

74. Riek, R., et al., *NMR characterization of the full-length recombinant murine prion protein, m PrP(23-231).* FEBS Letters, 1997. **413**(2): p. 282-288.

75. Zahn, R., et al., *NMR solution structure of the human prion protein.* Proc Natl Acad Sci U S A, 2000. **97**(1): p. 145-50.

76. Watt, N.T., et al., *Prion protein facilitates uptake of zinc into neuronal cells.* Nat Commun, 2012. **3**: p. 1134.

77. Turnbaugh, J.A., et al., *The N-terminal, polybasic region of PrP(C) dictates the efficiency of prion propagation by binding to PrP(Sc).* J Neurosci, 2012. **32**(26): p. 8817-30.

78. Millhauser, G.L., *Copper and the prion protein: methods, structures, function, and disease.* Annu Rev Phys Chem, 2007. **58**: p. 299-320.

79. Aronoff-Spencer, E., et al., *Identification of the Cu2+ binding sites in the N-terminal domain of the prion protein by EPR and CD spectroscopy.* Biochemistry, 2000. **39**(45): p. 13760-71.

80. Burns, C.S., et al., *Copper coordination in the full-length, recombinant prion protein.* Biochemistry, 2003. **42**(22): p. 6794-803.

81. Chattopadhyay, M., et al., *The octarepeat domain of the prion protein binds Cu(II) with three distinct coordination modes at pH 7.4.* J Am Chem Soc, 2005. **127**(36): p. 12647-56.

82. Walter, E.D., et al., *The prion protein is a combined zinc and copper binding protein: Zn2+ alters the distribution of Cu2+ coordination modes.* J Am Chem Soc, 2007. **129**(50): p. 15440-1.

83. Walter, E.D., M. Chattopadhyay, and G.L. Millhauser, *The affinity of copper binding to the prion protein octarepeat domain: evidence for negative cooperativity.* Biochemistry, 2006. **45**(43): p. 13083-92.

84. Varela-Nallar, L., et al., *Induction of cellular prion protein gene expression by copper in neurons.* Am J Physiol Cell Physiol, 2006. **290**(1): p. C271-81.

85. Brown, D.R., et al., *The cellular prion protein binds copper in vivo.* Nature, 1997. **390**(6661): p. 684-7.

86. Pushie, M.J., et al., *Prion protein expression level alters regional copper, iron and zinc content in the mouse brain.* Metallomics, 2011. **3**(2): p. 206-14.

87. Schmitt-Ulms, G., et al., *Evolutionary descent of prion genes from the ZIP family of metal ion transporters.* PLoS One, 2009. **4**(9): p. e7208.

88. Pauly, P.C. and D.A. Harris, *Copper stimulates endocytosis of the prion protein.* J Biol Chem, 1998. **273**(50): p. 33107-10.

89. Taylor, D.R., et al., *Assigning functions to distinct regions of the N-terminus of the prion protein that are involved in its copper-stimulated, clathrin-dependent endocytosis.* J Cell Sci, 2005. **118**(Pt 21): p. 5141-53.

90. Perera, W.S. and N.M. Hooper, *Ablation of the metal ion-induced endocytosis of the prion protein by disease-associated mutation of the octarepeat region.* Curr Biol, 2001. **11**(7): p. 519-23.

91. Watt, N.T., H.H. Griffiths, and N.M. Hooper, *Neuronal zinc regulation and the prion protein.* Prion, 2013. **7**(3): p. 203-8.

92. Evans, E.G., et al., *Interaction between Prion Protein's Copper-Bound Octarepeat Domain and a Charged C-Terminal Pocket Suggests a Mechanism for N-Terminal Regulation.* Structure, 2016. **24**(7): p. 1057-67.

93. Evans, E.G.B. and G.L. Millhauser, *Copper- and Zinc-Promoted Interdomain Structure in the Prion Protein: A Mechanism for Autoinhibition of the Neurotoxic N-Terminus.* Prog Mol Biol Transl Sci, 2017. **150**: p. 35-56.

94. McDonald, A.J., et al., *Altered Domain Structure of the Prion Protein Caused by Cu(2+) Binding and Functionally Relevant Mutations: Analysis by Cross-Linking, MS/MS, and NMR.* Structure, 2019. **27**(6): p. 907-922 e5.

95. Spevacek, A.R., et al., *Zinc drives a tertiary fold in the prion protein with familial disease mutation sites at the interface.* Structure, 2013. **21**(2): p. 236-46.

96. Thakur, A.K., et al., *Copper alters aggregation behavior of prion protein and induces novel interactions between its N- and C-terminal regions.* J Biol Chem, 2011. **286**(44): p. 38533-45.

97. Wu, B., et al., *The N-terminus of the prion protein is a toxic effector regulated by the C-terminus.* Elife, 2017. **6**.

98. Markham, K.A., et al., *Molecular Features of the Zn(2+) Binding Site in the Prion Protein Probed by (113)Cd NMR.* Biophys J, 2019. **116**(4): p. 610-620.

99. Martinez, J., et al., *PrP charge structure encodes interdomain interactions.* Sci Rep, 2015. **5**: p. 13623.

100. Sonati, T., et al., *The toxicity of antiprion antibodies is mediated by the flexible tail of the prion protein.* Nature, 2013. **501**(7465): p. 102-6.

101. Herrmann, U.S., et al., *Prion infections and anti-PrP antibodies trigger converging neurotoxic pathways.* PLoS Pathog, 2015. **11**(2): p. e1004662.

102. McDonald, A.J., B. Wu, and D.A. Harris, *An inter-domain regulatory mechanism controls toxic activities of PrP(C).* Prion, 2017. **11**(6): p. 388-397.

103. Coleman, B.M., et al., *Pathogenic mutations within the hydrophobic domain of the prion protein lead to the formation of protease-sensitive prion species with increased lethality.* J Virol, 2014. **88**(5): p. 2690-703.

104. Schatzl, H.M., et al., *Prion protein gene variation among primates.* J Mol Biol, 1995. **245**(4): p. 362-74.

105. Harris, D.A., et al., *Processing of a cellular prion protein: identification of N- and C-terminal cleavage sites.* Biochemistry, 1993. **32**(4): p. 1009-16.

106. Liang, J. and Q. Kong, *alpha-Cleavage of cellular prion protein.* Prion, 2012. **6**(5): p. 453-60.

107. McDonald, A.J. and G.L. Millhauser, *PrP overdrive: does inhibition of alpha-cleavage contribute to PrP(C) toxicity and prion disease?* Prion, 2014. **8**(2).

108. Kuffer, A., et al., *The prion protein is an agonistic ligand of the G protein-coupled receptor Adgrg6.* Nature, 2016. **536**(7617): p. 464-8.

109. Westergard, L., J.A. Turnbaugh, and D.A. Harris, *A naturally occurring C-terminal fragment of the prion protein (PrP) delays disease and acts as a dominant-negative inhibitor of PrPSc formation.* J Biol Chem, 2011. **286**(51): p. 44234-42.

110. Haigh, C.L. and S.J. Collins, *Endoproteolytic cleavage as a molecular switch regulating and diversifying prion protein function.* Neural Regen Res, 2016. **11**(2): p. 238-9.

111. Watt, N.T., et al., *Reactive oxygen species-mediated beta-cleavage of the prion protein in the cellular response to oxidative stress.* J Biol Chem, 2005. **280**(43): p. 35914-21.

112. Fischer, M., et al., *Prion protein (PrP) with amino-proximal deletions restoring susceptibility of PrP knockout mice to scrapie.* EMBO J, 1996. **15**(6): p. 1255-64.

113. Shmerling, D., et al., *Expression of amino-terminally truncated PrP in the mouse leading to ataxia and specific cerebellar lesions.* Cell, 1998. **93**(2): p. 203-14.

114. Baumann, F., et al., *Lethal recessive myelin toxicity of prion protein lacking its central domain.* EMBO J, 2007. **26**(2): p. 538-47.

115. Bremer, J., et al., *Axonal prion protein is required for peripheral myelin maintenance.* Nat Neurosci, 2010. **13**(3): p. 310-8.

116. Kovacs, T., et al., *Creutzfeldt-Jakob disease with amyotrophy and demyelinating polyneuropathy.* Arch Neurol, 2002. **59**(11): p. 1811-4.

117. Weckhuysen, D., et al., *Genetic Creutzfeldt-Jakob disease mimicking chronic inflammatory demyelinating polyneuropathy.* Neurol Neuroimmunol Neuroinflamm, 2015. **2**(6): p. e173.

118. Christensen, H.M. and D.A. Harris, *A deleted prion protein that is neurotoxic in vivo is localized normally in cultured cells.* J Neurochem, 2009. **108**(1): p. 44-56.

119. Li, A., et al., *Neonatal lethality in transgenic mice expressing prion protein with a deletion of residues 105-125.* EMBO J, 2007. **26**(2): p. 548-58.

120. Biasini, E., et al., *The toxicity of a mutant prion protein is cell-autonomous, and can be suppressed by wild-type prion protein on adjacent cells.* PLoS One, 2012. **7**(3): p. e33472.

121. Biasini, E., et al., *A mutant prion protein sensitizes neurons to glutamate-induced excitotoxicity.* J Neurosci, 2013. **33**(6): p. 2408-18.

122. Christensen, H.M., et al., *A highly toxic cellular prion protein induces a novel, nonapoptotic form of neuronal death.* Am J Pathol, 2010. **176**(6): p. 2695-706.

123. Massignan, T., E. Biasini, and D.A. Harris, *A Drug-Based Cellular Assay (DBCA) for studying cytotoxic and cytoprotective activities of the prion protein: A practical guide.* Methods, 2011. **53**(3): p. 214-9.

124. Solomon, I.H., et al., *An N-terminal polybasic domain and cell surface localization are required for mutant prion protein toxicity.* J Biol Chem, 2011. **286**(16): p. 14724-36.

125. Westergard, L., J.A. Turnbaugh, and D.A. Harris, *A nine amino acid domain is essential for mutant prion protein toxicity.* J Neurosci, 2011. **31**(39): p. 14005-17.

126. Solomon, I.H., J.E. Huettner, and D.A. Harris, *Neurotoxic mutants of the prion protein induce spontaneous ionic currents in cultured cells.* J Biol Chem, 2010. **285**(34): p. 26719-26.

127. Massignan, T., et al., *A novel, drug-based, cellular assay for the activity of neurotoxic mutants of the prion protein.* J Biol Chem, 2010. **285**(10): p. 7752-65.

128. Fang, C., et al., *Prions activate a p38 MAPK synaptotoxic signaling pathway.* PLoS Pathog, 2018. **14**(9): p. e1007283.

129. Solomon, I.H., E. Biasini, and D.A. Harris, *Ion channels induced by the prion protein: mediators of neurotoxicity.* Prion, 2012. **6**(1): p. 40-5.

CHAPTER 2

Intrinsic Toxicity of the Cellular Prion Protein is Regulated by its Conserved Central Region

Graham P. Roseman, Bei Wu, Mark A. Wadolkowski, David A. Harris, Glenn L. Millhauser

Introduction

Transmissible spongiform encephalopathies, also known as prion disorders, are a class of neurodegenerative diseases that occur due to misfolding of the mainly α-helical cellular prion protein (PrP^C) into the ß-sheet rich PrP scrapie isoform (PrP^{Sc}) [1, 2]. Prion diseases include Creutzfeldt-Jakob disease (CJD) and Gerstmann–Sträussler–Scheinker syndrome (GSS) in humans, Mad Cow disease in bovine. The neurotoxicity found in prion diseases is dependent on the host's expression of PrP^C [3]. PrP^C is natively found as a glycosylphosphatidylinositol (GPI) anchored glycoprotein located on the extracellular side of the plasma membrane and associated with lipid rafts [4]. PrP^C is expressed ubiquitously throughout the brain and enriched in neurons [5-7].

Mature PrP^C is composed of 208 amino acids (mouse numbering: residues 23-230), distributed over two major domains. The globular C-terminal domain (residues 126-230) consists of three α-helices and one short anti-parallel ß-sheet, collectively stabilized by a disulfide bond [8]. The partially structured N-terminal domain (residues 23-104) contains several functional segments. Among these are the octarepeat (OR) segment ($(PHGG(G/S)WGQ)_4$; residues 59-90), that takes up copper and zinc at physiological concentrations [9-13] and the polybasic N-terminus (residues 23-31), both asserting regulatory control over certain transmembrane receptors. For example, Zn^{2+}- and Cu^{2+}-binding to the OR modulates AMPA receptor (AMPAR) activity [14] and NMDA receptor activity [15], respectively. More generally,

expression levels of PrP^C in mice alters the anatomic distribution of Zn^{2+} and Cu^{2+} throughout the brain [16].

Recent studies find that the partially structured N-terminus and the globular C-terminal domains of PrP^C directly interact [17, 18]. This *cis*-interdomain interaction is mediated by both Zn^{2+} [19] and Cu^{2+} [18, 20-22] binding to the OR domain as well as electrostatic interactions between the polybasic N-terminus and a negatively charged patch on the globular C-terminal domain [22-24]. These results are of interest due to recent literature describing neurotoxicity driven by antibodies, such as POM1, that target the C-terminal domain of PrP^C [25], generating cellular responses similar to that elicited by administration of PrP^{Sc} such as generation of reactive oxygen species, activation of unfolded protein response, and downregulation of similar genes [26]. Specifically, the POM1 epitope is located to the PrP^C C-terminal surface that stabilizes the metal ion-promoted, protective *cis*-interaction [17, 20]. Interestingly, the toxicity elicited by C-terminal antibodies [18] is blocked by the co-administration of N-terminal antibodies [25], which suggests that the N-terminus of PrP^C is a toxic effector domain regulated by the globular C-terminal domain. Remarkably, N-terminal antibodies are able to reduce PrP^{Sc}-induced toxicity in cerebral organotypic slices [26], further suggesting the toxic potential of the N-terminus of PrP^C.

The intervening linker connecting the two major domains is called the central region (CR) (residues 105-125) and is highly conserved among mammalian species [27, 28]. Notably, in healthy tissues this region is a locus for proteolysis, termed α-cleavage

[29, 30] that generates a N-terminal fragment (N1) and a membrane bound C-terminal domain (C1), both having proposed biological functions [31, 32]. In addition to cleavage, the CR along with the polybasic N-terminus are high affinity docking sites for amyloid beta (Aß) oligomers [33, 34].

Developing a mechanistic understanding of the toxicity elicited by the prion protein is of the upmost importance since cell surface expression of this species transmits toxic transmembrane signals in both prion and Alzheimer's disease. Over the years, insight into the mechanisms come from deletions targeted to the CR. It was initially reported in transgenic mice that Δ32-134 PrP^C (ΔF PrP^C) generates spontaneous neurodegeneration and death within 2-5 months which is reversed upon the coexpression of WT PrP^C [35]. Later it was found that retaining more of the N-terminus of PrP^C (Δ94-134) results in myelin degeneration and death within 20-30 days [36]. Paradoxically, the shortest studied deletion encompassing just the short CR, Δ105-125 (ΔCR PrP^C), leads to the most severe neurodegenerative phenotype, with consequent fatality about one week after birth [37, 38].

Due to its profound neurotoxicity, ΔCR PrP^C has been the focus of numerous recent investigations [18, 22, 37, 39-45]. ΔCR PrP^C is trafficked and localized to the extracellular membrane similar to WT PrP^C [40]. In cell culture, whole cell electrophysiological patch clamp experiments find that ΔCR PrP^C induces large inward spontaneous currents [41, 45] which correlate with a decrease in cellular viability in a drug-based cellular assay (DBCA) [46]. Both spontaneous currents and drug-induced

toxicities can be blocked by the concurrent overexpression of WT PrP^C or by deletion of the polybasic N-terminus in ΔCR PrP^C [47]. Interestingly, these currents are also induced in WT PrP^C expressing cells with C-terminal antibodies [18], paralleling the C-terminal antibody experiments previously described. Additionally, C-terminal antibody and ΔCR PrP^C induced currents can be blocked by co-administration of N-terminal antibodies or N-terminal ligands (e.g. Cu^{2+}) [18, 48]. These results point towards the CR at playing a central role in regulating the toxic N-terminus – a role that may unify the disparate PrP^C dependent modes of neurotoxicity.

Despite the focus on ΔCR PrP^C neurodegeneration, the mechanism by which the CR regulates the toxic N-terminus is unknown. It has been thought previously that the CR is simply a passive linker between the metal binding N-terminus and the globular domain. Opposing this view is the observation that the CR sequence is highly conserved and, as noted above, its deletion causes neonatal fatality in transgenic mice and spontaneous currents in cell culture. Two possible explanations can be envisioned to explain the role of the CR: (1) this region is necessary to facilitate the metal-driven *cis*-interaction; and (2) it is required because it is the locus for α-cleavage. In the absence of either or both of these functions of the CR, PrP^C may acquire toxic activities. The aim of this study was to use protein design, NMR, electrophysiology, cleavage assays, cellular crosslinking, and cell survival studies to fully investigate the role of the CR in PrP^C structure and toxicity of ΔCR PrP^C. Our results demonstrate that the CR is not a passive linker between the N- and C-terminal domains. Instead, we find

that the CR facilitates PrP^C-PrP^C dimerization or in some other fashion provides conformational control over the proteins toxic N-terminal segment, thereby serving as a regulator of PrP^C-mediated neurotoxicity.

Materials and Methods

Plasmids

pcDNA3.1(+) Hygro plasmids (Invitrogen) encoding WT and ΔCR PrP^C used for mammalian cell transfections have been described previously [41, 43, 49]. pJ414 vector (DNA2.0) encoding WT PrP^C used for recombinant protein expression has been previously described [20]. To generate the vectors for G5, $G5_{\alpha1}$, $G5_{\alpha23}$, and His to Ala PrP^C (both for the PCDNA 3.1 (+) Hyrgo plasmid and pj414 vector), Gibson cloning was used [50]. Briefly, primers were purchased from Invitrogen to linearize the plasmid while deleting out the selected area to be replaced using Phusion® High-Fidelity PCR Master Mix (New England Biolabs®). Linearization reactions were run on a 1% agarose gel and linearized DNA was extracted with GeneJET Gel Extraction Kit (Thermo Fisher Scientific). Gibson reactions were run using Gibson Assembly® Master Mix (New England Biolabs®) and transformed into E. coli (DH5α(DE3) Invitrogen). Colonies were grown and pure DNA was extracted using Qiagen Mini prep kits. Constructs were then verified by DNA sequencing. Plasmids used in mammalian cell culture were further grown and purified using GenElute™ HP Endotoxin-Free Plasmid Maxiprep Kit (Sigma-Aldrich®). Point mutations were introduced using PCR-based site-directed

mutagenesis with mutagenic primers (Invitrogen) and Phusion® High-Fidelity PCR Master Mix (New England Biolabs®). Constructs were verified by DNA sequencing.

Cell Lines

HEK 293T cells (ATCC® CRL-3216™, Lot # 62729596) were maintained in high glucose DMEM supplemented with 10% fetal bovine serum (Life Technologies) and GlutaMAX (Gibco). PrP^C knockout (PrPKO) N2a cells have been described previously [51]. PrPKO N2a cells were maintained in low glucose DMEM supplemented with nonessential amino acids (Corning), 10% heat-inactivated fetal bovine serum (Life Technologies), GlutaMAX, and MycoZap™ Plus-CL (Lonza). HEK 293T and PrPKO N2a cell lines used in this study were mycoplasma free and were maintained at 37 ^oC in a 5% carbon dioxide incubator.

HEK 293T cells and PrPKO N2a cells used for western blotting were transiently transfected using LipoD293™ In Vitro DNA Transfection Reagent (SignaGEN® Laboratories) with PrP^C encoding pcDNA3.1(+)Hygro plasmids in 6-well plates. Fifteen to eighteen hours after cells were transfected, the media was changed and cells were allowed to recover for 24 hours. PrPKO N2a cells used for electrophysiology were transiently transfected using Lipofectamine 2000 with pEGFP-N1 (Clontech).

Cell preparation and Western Blotting

Whole cell lysates were prepared by washing cells 2x with PBS. Cells were then lysed with lysis buffer (50 mM tris(hydroxymethyl)aminomethane (Tris) (pH 8), 150 mM sodium chloride (NaCl), 1 mM ethylenediaminetetraacetic acid (EDTA), 1% Triton X-100, 10% Glycerol, supplemented with Halt™ Protease Inhibitor Cocktail (Thermo Fisher Scientific)) and quantified using Pierce™ BCA Protein Assay Kit (Thermo Fisher Scientific). To remove N-linked glycans, cell lysates were treated with recombinant PNGase F (New England Biolabs®) under denaturing conditions according to the manufacturers protocol. Completed PNGaseF reactions were boiled in SDS-PAGE buffer and run on a 4–20% Mini-PROTEAN® TGX™ Precast Protein Gels (Bio-Rad) along with Precision Plus Protein™ WesternC™ Blotting Standards (Bio-Rad). SDS-PAGE gels were subsequently washed with water three times totaling 15 minutes and transferred to a nitrocellulose membrane using Trans-Blot® Turbo™ Transfer System (Bio-Rad). Membranes were blocked using 5% bovine serum albumin in TBS-T. PrP^C constructs were probed with PrP^C Antibody (M-20) (Santa Cruz Biotechnology, sc-7694, goat origin) who's epitope matches near the C-terminus of PrP^C. The PrP^C antibody was then detected with HRP Rabbit Anti-Goat IgG (Abcam: ab6741) and the ladder was detected with Precision Protein™ StrepTactin-HRP Conjugate (Bio-Rad). Blots were exposed to Pierce™ ECL Western Blotting Substrate (Thermo Fisher Scientific) and images were taken using ChemiDoc™ XRS+ System (Bio-Rad) and analyzed using Image Lab™ Software (Bio-Rad).

Cell surface PrP^C was analyzed by treating transfected cells with 0.1 units Phosphatidylinositol-Specific Phospholipase C Protein (PIPLC) (Life Technologies) in 200 µL phosphate buffered saline (PBS) (+,+) rocking gently for two hours at 4 °C. Supernatants containing released PrP^C were collected were spun at 300 x g for five minutes at 4 °C to pellet any cells that were dislodged from the plate. Supernatants were then transferred to a separate tube and glycerol was added to a final concentration of 5%. SDS-PAGE samples were prepared by adding non-reducing SDS-PAGE sample buffer and boiling for five minutes. SDS-PAGE gels and western blots were run as described above.

Protein Expression

Recombinant PrP constructs encoding the various mouse PrP^C(23-230) constructs in the pJ414 vector (DNA 2.0) were transformed into and expressed using *E. coli* (BL21 (DE3) Invitrogen) [20]. Bacteria was grown in M9 minimal media supplemented with $^{15}NH_4Cl$ (1 g/L) (Cambridge Isotopes) for ^1H-^{15}N HSQC experiments or in LB media (Research Product International). Cells were grown at 37°C until reaching an optical density (OD) of 1-1.2, at which point expression was induced with 1 mM isopropyl-1-thio-D-galactopyranoside (IPTG). PrP^C constructs were purified as previously described [19]. Briefly, proteins were extracted from inclusion bodies with extraction buffer (8 M guanidium chloride (GdnHCl), 100 mM Tris, 100 mM Sodium Acetate (pH 8)) at room temperature and were purified by Ni^{2+}-

immobilized metal-ion chromatography (IMAC). Proteins were eluted from the IMAC column using elution butter (5 M GdnHCl, 100 mM Tris, 100 mM Sodium Acetate (ph 4.5)) and were brought to pH 8 with 6 M potassium hydroxide (KOH) and left at 4°C for 2 days to oxidize the native disulfide bond. Proteins were then desalted into 50 mM potassium acetate buffer (pH 4.5) and purified by reverse-phase HPLC on a C_4 column (Grace). Pure protein was lyophilized and stored at -20 ^{o}C until needed. The purity and identity of all constructs were verified by analytical HPLC and mass spectrometry (ESI-MS). Disulfide oxidation was confirmed by reaction with N-ethylmaleimide and subsequent ESI-MS analysis.

NMR

Lyophilized uniformly ^{15}N-labeled PrP^{C} constructs were first suspended in water until fully solubilized and concentrations were checked using the absorbance at 280 nm (A_{280}) with the proper extinction coefficient. NMR samples were made to 300 µM in 10 mM 2-(*N*-morpholino)ethanesulfonic acid (MES) buffer with 10% D_2O and the pH was adjusted to 6.1 with 600 mM hydrochloric acid. Apo samples were loaded into a Shigemi NMR tube (Wilmad Glass, BMS-005B) and a ^{1}H- ^{15}N HSQC spectrum as collected at 37 ^{o}C on an 800-MHz spectrometer (Bruker, Billerica, MA) at the University of California, Santa Cruz NMR Facility (Santa Cruz, CA). The sample was then removed from the tube and one equivalent of Cu^{2+} from a 10 mM copper chloride solution in water (determined accurately by flame atomic absorption) was added and

the pH was adjusted to 6.1 if necessary. The sample was loaded back into the Shigemi NMR tube and the sample height was adjusted to match the sample height of the apo sample and another ^{1}H- ^{15}N HSQC spectrum was collected. NMR spectra were analyzed with NMRPipe [52] and Sparky. Structural analysis was performed with Chimera [53]. Protein assignments were achieved using previously determined values [20].

ADAM8 Cleavage Assay

ADAM8, ADAM10, and ADAM17 were purchased from R&D systems. ADAM8 was activated according to the manufactures protocol. Activated ADAM8 was then diluted into ADAM8 dilution buffer (20 mM Tris, 5 mM calcium chloride ($CaCl_2$), and 25mM potassium chloride (KCl) (pH 7.4), aliquoted, flash frozen in liquid nitrogen, and stored at -80 ^{o}C until needed. ADAM10 and ADAM17 were diluted into ADAM10 assay buffer (25mM Tris, 2.5 µM zinc chloride, and 0.005% Brij-35 (pH 7.4)), aliquoted, flash frozen in liquid nitrogen, and stored at -80 ^{o}C until needed.

Working stocks of purified PrP^{C} were prepared to 40 µM in ADAM8 dilution buffer (for ADAM8 assay) or ADAM10 assay buffer (ADAM10 or ADAM17 assay). Cleavage assays were previously described by McDonald et. al. Briefly, assays were set up by mixing 15 µL PrP^{C} and 15 µL ADAM protease and reacted overnight at 37 ^{o}C. Reactions were quenched by the addition of 5 µL 1% formic acid and stored on ice or at 4 ^{o}C until needed. 30 µL of the supernatant were pipetted into autosampler vials and loaded

into an LTQ LC/MS autosampler (Thermo Fisher Scientific). 20 µL of cleavage products was drawn from the vial and separated with a C_4 HPLC column (Higgins Analytical) using a 60-min gradient of water/acetonitrile mobile phases. The A_{280} was continuously recorded by a photodiode array, whereas mass spectra were continuously taken using an LTQ mass spectrometer (Thermo Fisher Scientific). The C_4 column was flushed with 95% acetonitrile to remove any residually bound protein and then re-equilibrated with 95% water between each sample run.

The LC/MS spectra from each sample run were first analyzed by MS Bioworks. The mass spectrum ladder for each peak separated by the C_4 column was deconvoluted using Bioworks to reveal the parent mass of the cleavage product (data not shown). The masses of the observed peaks were cross-referenced against the predicted masses of hydrolysis of all possible peptide bonds of the particular PrP^C construct being assayed to determine which cleavage product was produced. For all cleavage fragments enzymatically produced, observed masses were within 1 atomic mass unit of the mass of a predicted cleavage fragment.

Cell Viability Assay using WST-1

The cell viability assay conducted was described previously [42] and adapted for this study. 96-well plates for were seeded with 1 x 10^4 cells in 100 µL high glucose DMEM and grown overnight. Wells were transfected with 50 ng of PrP^C DNA using LipoD293™ In Vitro DNA Transfection Reagent (SignaGEN® Laboratories). Media was

changed 18 hours later and replaced with either DMEM or DMEM supplemented with G418 (Life Technologies) and cells were allowed to grow for 48 hours. After this time 10 µL of Cell Proliferation Reagent WST-1 (Roche) was added to each well and allowed to incubate at 37 ^{o}C for 1-2 hours. After this time, the A_{450} was measured for each well using a Perkin-Elmer EnVision plate reader. Background subtractions were made by subtracting the A_{450} of well with just DMEM and 10 µL WST-1 reagent from the A_{450} of the sample wells. Viability was measured by dividing the A_{450} value of the G418 treated cells by the A_{450} of the untreated cells.

Electrophysiology

Recordings were made from PrPKO N2a cells 24–48 hours after transfection. Transfected cells were recognized by green fluorescence resulting from co-transfection with pEGFP-N1. Whole-cell patch clamp recordings were collected using standard techniques. Pipettes were pulled from borosilicate glass and polished to an open resistance of 2–5 megaohms. Experiments were conducted at room temperature with the following solutions: internal, 140 mM cesium-glucuronate, 5 mM cesium chloride, 4 mM magnesium-ATP, 1 mM disodium-GTP, 10 mM ethylene glycol-bis(β-aminoethyl ether)-N,N,N',N'-tetraacetic acid (EGTA), and 10 mM 4-(2-hydroxyethyl)-1-piperazineethanesulfonic acid (HEPES) (pH 7.4 with cesium hydroxide); external, 150 mM NaCl, 4 mM KCl, 2 mM $CaCl_2$, 2 mM magnesium chloride ($MgCl_2$), 10 mM glucose, and 10 mM HEPES (pH 7.4 with NaOH). Current signals were

collected from a Multiclamp 700B amplifier (Molecular Devices, Sunnyvale, CA), digitized with a Digidata 1440 interface (Molecular Devices), and saved to disc for analysis with pCLAMP™ 10 software.

Results

Blocking cis-interaction does not elicit toxicity

Deletion of the CR leads to a weakening of the Cu^{2+}-driven *cis*-interaction [18] as well as elimination of α-cleavage [30]. Either of these two major changes could lead to the spontaneous neurotoxicity. To investigate whether neurotoxicity is due to a weakened Cu^{2+}-driven *cis*-interaction, His to Ala PrP^{C} was designed in which all of the histidine's within the OR were mutated to alanine's (Figure 1B). By deleting out the OR histidine's, the OR cannot bind Cu^{2+}, in turn eliminating the primary driving force for the *cis*-interaction [17].

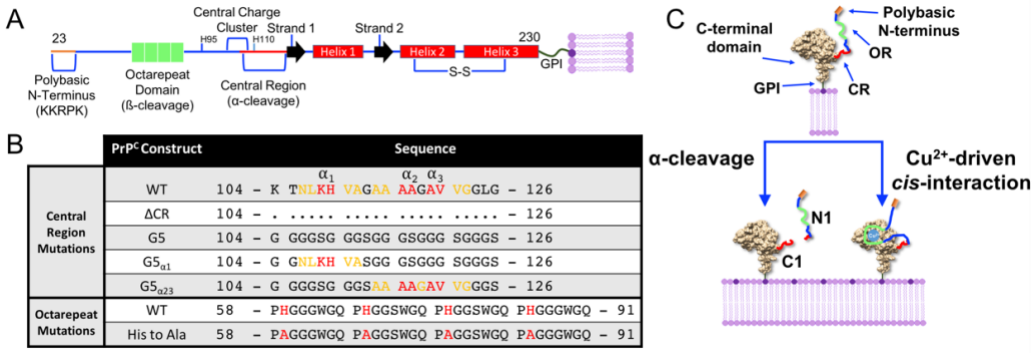

Figure 8: **Schematic of PrP^C. A.** Linear schematic of PrPC. **B.** Sequences used in this study. CR mutations were made to modulate α-cleavage. In the CR mutation panel, the residues highlighted in red are where α-cleavage occurs between (α1-α3). Residues highlighted in orange are the P3'-P2' or P3-P2 relative to the cleavage site. In the OR mutation panel, the residues highlighted in red are the histidine residues that Cu^{2+} bind to (WT PrPC) or what those histidine residues were mutated to in His to Ala PrPC. **C.** Two regulatory process of PrPC. PrPC can undergo α-cleavage to generate a released N1 fragment and the membrane C1 fragment. Additionally, the binding of Cu^{2+} to the OR drives a domain-domain cis-interaction between the Cu^{2+}-bound OR and the globular C-terminal domain. The CR is shown in red. The OR is shown in green. The polybasic N-terminus is shown in orange.

To ensure His to Ala PrP^C undergoes α-cleavage to a similar extent as WT PrP^C, both constructs were transfected into either HEK293T cells or PrP knock out (PrPKO) N2a cells (Figure 2A-B). Whole cell lysates were treated with PNGaseF to remove N-linked glycans and analyzed by western blot. Both WT and His to Ala PrP^C displayed two main bands, one corresponding to full-length protein (FL) and the other corresponding to the C-terminal fragment generated by α-cleavage (C1). Quantitating the intensity of the C1 band revealed that His to Ala PrP^C (48 ± 6.7% and 27 ± 8.8% C1 band in HEK293T and PrPKO N2a cells, respectively) was cleaved to a similar extent as WT PrP^C (37 ± 8.1% and 32 ± 0.6% C1 band in HEK293T and PrPKO N2a cells, respectively).

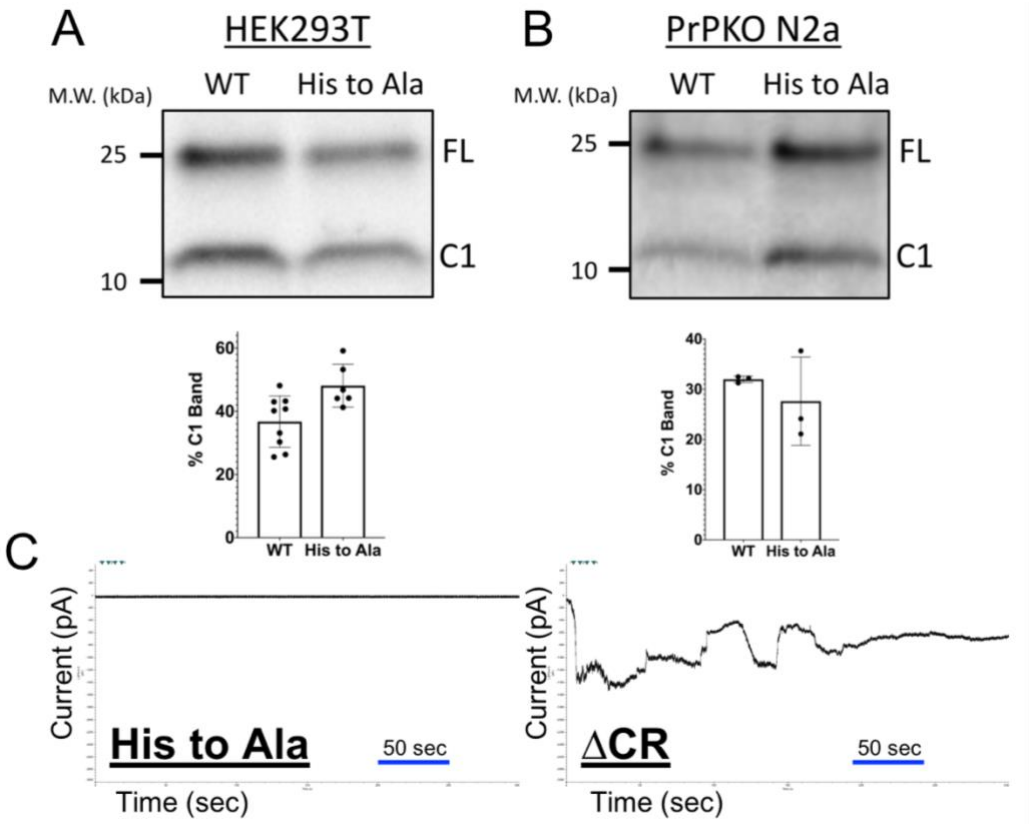

Figure 9: **Mutating the OR histidine's to alanine's (His to Ala PrP^C) retains cleavage in cells and does not drive spontaneous currents**. Western blots of PNGaseF treated lysates of HEK293T cells **(A)** or N2a cells **(B)** transfected with either WT or His to Ala PrP^C. Uncleaved full length band is denoted by FL and the C-terminal side of α-cleavage is denoted by C1. The bar graph below each blot show the quantitation by densitometric analysis of %C1 band relative to the sum of FL and C1 bands. Error bars represent ± S.D. from at least three independent experiments. In both cell lines, α-cleavage of His to Ala PrP^C is comparable to WT PrP^C. **C.** Representative current recordings of either His to Ala or ΔCR PrP^C transfected PrPKO N2a cells show that His to Ala PrP^C does not have spontaneous currents.

Whole cell patch clamp experiments were conducted on PrPKO N2a cells held at -70 mV to test if inward currents were generated by blocking the metal-driven *cis*-interaction (Figure 2C). ΔCR PrP^C transfected cells displayed strong inward spontaneous currents which is in agreement with a previous study [41]. In contrast, His to Ala PrP^C transfected cells did not show large inward currents. This demonstrates that eliminating Cu^{2+} binding to the OR is not sufficient enough to produce ΔCR PrP^C-like currents. It can then be inferred that there must be other factors leading to the

currents generated by ΔCR PrP^C than loss of the *cis*-interaction facilitated by histidine residues in the OR. This is in agreement with previous studies showing deletion of the OR (ΔCR/Δ59-90) has no effect on the magnitude of the currents generated relative to ΔCR PrP^C [18, 43].

Blocking cleavage with flexible linker generates currents

ΔCR PrP^C lacks the stretch of 21 highly conserved amino acids that encompass the α-cleavage sites (Figure1). A previous *in vitro* study showed that there are multiple α-cleavage sites within the CR (α_1-α_3, Figure 1B). Proteolysis within this segment separates the N-terminal domain, resulting in a putative loss of intrinsic PrP^C function [30, 54]. To address the possibility that the toxicity of ΔCR PrP^C is due to misregulation from loss of α-cleavage, the WT PrP^C CR was replaced with a flexible glycine-serine-rich linker (G5 PrP^C, Figure 1). This glycine-serine rich linker was chosen for its solubility and high degree of flexibility to allow for the Cu^{2+}-driven *cis*-interaction in addition to its resistance to proteolysis [55].

To investigate if G5 PrP^C retains the Cu^{2+}-driven *cis*-interaction, paramagnetic relaxation enhancement NMR was employed [20]. With the intrinsic paramagnetism of Cu^{2+}, resulting from its d^9 electron configuration, there is an increase in the relaxation rate of the NMR active nuclei when Cu^{2+} is in close proximity. This causes a broadening and a decrease in the intensity of the resonance lines which is inversely proportional to the distance of Cu^{2+} to the backbone amide bond. Uniformly ^{15}N-

labeled protein was prepared and ^{1}H-^{15}N HSQC spectra were collected in the absence and presence of 1 eq. of Cu^{2+}. The intensity of the resonance cross peaks with 1 eq. of Cu^{2+} (I) was divided by the intensity of the resonances in the absence of Cu^{2+} (I_o) to generate intensity ratios (I/I_o) for each backbone NH. I/I_o vs. residue plots were made for both WT PrP^C and G5 PrP^C comprising amino acids 126-230 (Figure 3A). Residues considered strongly affected by the addition of Cu^{2+} (those that are affected by greater than 1σ) are shown in blue on the surface representations of the PrP^C C-terminal domain (PDB: 1XYX) below each intensity ratio plot. The residues affected localize to three main patches: the C-terminal end of the loop going into helix 1 (Patch 1), the N-terminal end of helix 2 (Patch 2), and the N-terminal half of helix 3 (Patch 3). Both WT and G5 PrP^C show similar residue-specific patterns demonstrating that G5 PrP^C retains the Cu^{2+}-driven *cis*-interaction.

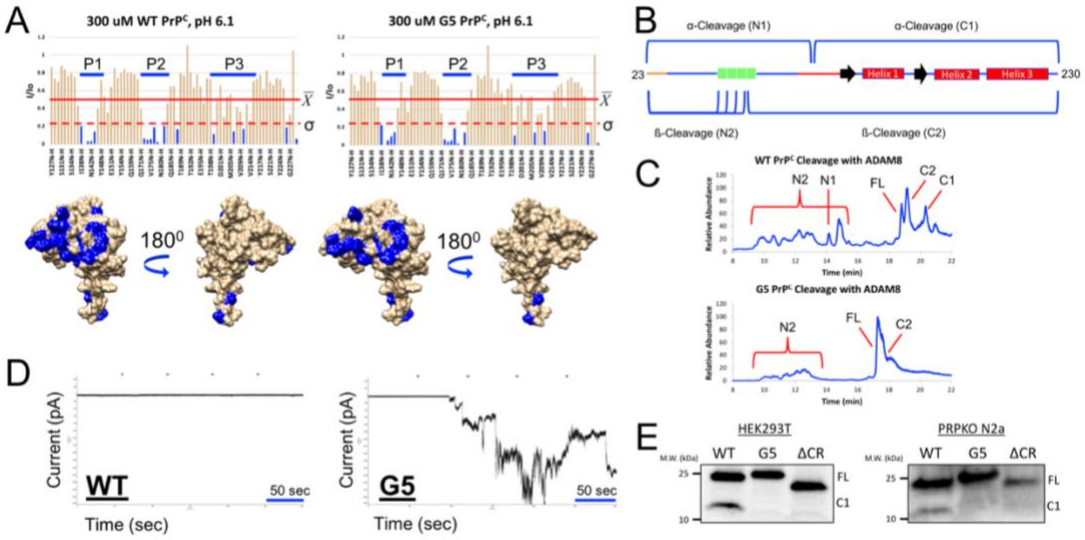

Figure 10: **Mutating the CR to a flexible GS linker retains the copper-driven cis-interaction, blocks alpha cleavage, and generates spontaneous currents**. **A.** I/I_o vs. residues plot of WT or G5 PrP^C constructs titrated with 1eq. of Cu^{2+} at pH 6.1 and 37 ^oC. The average ($\bar{X}$) and standard deviation (σ) of only similar residues of each construct were taken. Below each plot is the surface representation of the C-terminus of PrP^C (PDB: 1XYX). Residues in blue are the residues where the I/I_o values are affected by greater than one standard deviation. Both WT and G5 PrP^C constructs have similar residues affected to a similar degree, thus the cis-interaction is retained. **B.** Schematic diagram of PrP^C showing the possible cleavage products that can be produced from in vitro cleavage assays. **C.** LC/MS traces of in vitro cleavage assays using recombinant WT or G5 PrP^C constructs reacted with ADAM8 overnight at 37 ^oC. Reactions were loaded onto a C8 column and were eluted using a gradient of water and acetonitrile. When analyzed using the LC/MS, WT PrP^C produces α- and ß-cleavage where G5 PrP^C produces only ß-cleavage.
D. Representative current recordings of either WT or G5 PrP^C transfected PrPKO N2A cells. The data shows that G5 PrP^C has spontaneous currents, which are characteristic of toxicity. **E.** Western blots of PNGaseF treated lysates of HEK293T or PrPKO N2a cells transfected with DNA coding for either WT, ΔCR, or G5 PrP^C. Uncleaved full length protein is denoted by FL and the C-terminal side of α-cleavage is denoted by C1. In HEK293T cells, WT PrP^C produces only α-cleavage, where ΔCR and G5 PrP^C did not undergo any cleavage events. In PrPKO N2a cells, WT PrP^C underwent α-cleavage, where ΔCR and G5 PrP^C were not cleaved at all.

To investigate if G5 PrP^C can undergo α-cleavage, HEK293T or PrPKON2a cells were transfected with WT, G5, or ΔCR PrP^C. PNGaseF treated lysates were analyzed by western blot (Figure 3E). Results show that G5 and ΔCR PrP^C did not undergo α-cleavage. Cleavage assays using ADAM8 protease, the protease responsible for α-cleavage in skeletal muscle [30, 56], were undertaken with recombinant PrP^C to test

if G5 PrP^C can be cleaved *in vitro* (Figure 3C). Results showed that G5 PrP^C underwent ß-cleavage in the OR region, which agrees with a previous study [30]. In contrast, G5 PrP^C is not susceptible to α-cleavage in ADAM8 assays, supporting the primary design goal for this construct.

Electrophysiology measurements were then performed to test if blocking α-cleavage induces currents as seen with ΔCR PrP^C (Figure 2D). PrPKO N2a cells were transfected with WT PrP^C did not display inward currents. Conversely, G5 PrP^C transfected cells produced large inward currents. These results suggest that blocking α-cleavage by introduction of the G5 linker may be responsible for inducing inward currents similar to ΔCR PrP^C.

Reintroduction of α-cleavage in G5 PrP^C generates currents

If the currents generated by G5 PrP^C are due to blockage of α-cleavage, then inward currents should be eliminated upon reintroduction of cleavage into the G5 linker. $G5_{\alpha1}$ PrP^C was designed by reintroducing α_1-cleavage in the G5 linker (Figure 1B). ADAM8 cleavage assays (Figure 4D) and PNGaseF treated cell lysates (Figure 4A-B) show that $G5_{\alpha1}$ PrP^C regains α-cleavage (38 ± 5.6% and 31 ± 6.6% C1 band in HEK293T and PrPKO N2a cells, respectively). Due to the close proximity of α_2 and α_3 in the linear sequence, $G5_{\alpha23}$ PrP^C was designed which simultaneously adds back both cleavage sites (Figure 1B). In contrast to $G5_{\alpha1}$ PrP^C, $G5_{\alpha23}$ PrP^C exhibited no α-cleavage

in vitro and in cells (Figure 4A-B, D). These results show that with the cell lines used, PrP^C undergoes α-cleavage at the α_1-cleavage sites.

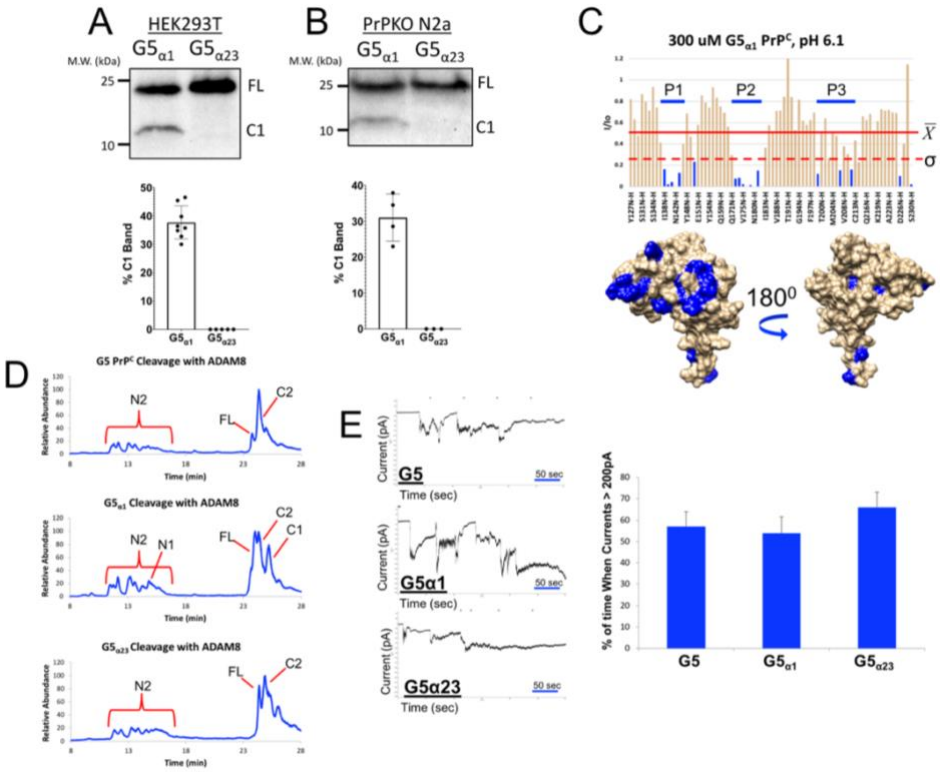

Figure 11: **Addition of α-cleavage (α_1 or α_{23}) site back into G5 PrP^C still generates spontaneous currents**. Western blots of PNGaseF treated lysates of HEK293T cells **(A)** or PrPKO N2a cells **(B)** transfected for either $G5_{\alpha1}$ or $G5_{\alpha23}$ PrP^C constructs. The bar graph below each blot show the quantitation by densitometric analysis of %C1 band relative to the sum of FL and C1 bands. Error bars represent ± S.D. from at least three independent experiments. In HEK293T cells, $G5_{\alpha1}$ PrP^C regains α-cleavage where $G5_{\alpha23}$ PrP^C does not. However, in PrPKO N2a cells, both constructs have α- and ß-cleavage. **C.** I/I_o vs. residues plot of recombinant $G5_{\alpha1}$ PrP^C with 1eq. of Cu^{2+} at pH 6.1 and 37 °C. The average (X) and standard (σ) deviation were taken. Below the plot is the surface representation of the C-terminus of PrP^C (PDB: 1XYX). Residues in blue are the residues where the I/I_o values are affected by greater than one standard deviation. $G5_{\alpha1}$ PrP^C has similar residues affected to a similar degree as WT PrP^C, thus the cis-interaction is retained. **D.** LC/MS traces of in vitro cleavage assays using recombinant G5, $G5_{\alpha1}$, or $G5_{\alpha23}$ PrP^C constructs were reacted with ADAM8 overnight at 37 °C. Reactions were quenched with formic acid to a final concentration of 3% and then 10 µg of PrP^C was loaded onto a C8 column. Cleavage products were eluted using a gradient of water and acetonitrile. When analyzed using LC/MS. $G5_{\alpha1}$ PrP^C produces α- and ß-cleavage where G5 and $G5_{\alpha23}$ produces only ß-cleavage. **E.** Representative current recordings of either G5, $G5_{\alpha1}$, or $G5_{\alpha23}$ PrP^C transfected PrPKO N2a cells. The bar graph next to the current recording is the quantitation of the time the currents are greater than 200pA. Error bars represent ± S.E.M from at least three different independent experiments. The data shows that even though α-cleavage is regained in $G5_{\alpha1}$ PrP^C, spontaneous currents are still generated.

Electrophysiology experiments were then conducted to test if adding back susceptibility to α-cleavage reduces the generated inward currents (Figure 4E). Both $G5_{\alpha1}$ and $G5_{\alpha23}$ PrP^C transfected PrPKO N2a cells still exhibit large inward current. Quantification of the data (measured by the percentage of time the currents exceeded 200 pA) revealed that G5, $G5_{\alpha1}$, and $G5_{\alpha23}$ PrP^C generated the same time-averaged currents. This result demonstrates that the large inward currents, which are highly correlated with toxicity in animals, still persists even when PrP^C retains susceptibility to α-cleavage.

Cleavage of the N-terminus, without replenishment of cell surface PrP^C, must decrease the magnitude of the currents generated since it removes the polybasic extreme N-terminus responsible for current activity [43]. If cell surface $G5_{\alpha1}$ PrP^C was cleaved with an efficiency of 20-40%, then the currents should show a concomitant decrease of approximately the same amount, which is not observed in our analysis. However, when quantitating the percentage of time the currents are significant, a threshold current value was chosen. Therefore, it is possible that $G5_{\alpha1}$ PrP^C exhibits a weaker current magnitude than G5 PrP^C, but it spends the same amount of time over the threshold current value as G5 and $G5_{\alpha23}$ PrP^C. Our results are nevertheless significant since they demonstrate that the full length $G5_{\alpha1}$ PrP^C remaining on the cell surface still generates potent currents similar to ΔCR PrP^C. Additionally, WT PrP^C on the cell surface is mostly full length, but it contains the CR. Thus there is something

intrinsically encoded into the WT CR sequence that is able to attenuate the toxicity of the N-terminus.

The CR sequence facilitates dimerization

Results thus far show that the inward currents measured in the electrophysiology experiments are not a result of a weakened Cu^{2+}-promoted *cis*-interaction or from blocking α-cleavage. This suggests that there is something inherent to the sequence of the CR that regulates the toxic N-terminus thereby muting inherent PrP^C toxicity. In addition to conservation of this segment, the CR is notable for its high content of hydrophobic and small aliphatic amino acids. It was previously demonstrated that a peptide consisting of residues 105-125 readily forms fibrils that are toxic to cells if they express membrane anchored WT PrP^C [57]. Given that PrP(105-125) binds to PrP^C suggests that the CR of proximal PrP^C monomers may facilitate inter-PrP^C interactions. In support of this, a previous study using cross-linkable unnatural amino acids in recombinant protein demonstrated that dimerization is facilitated by the CR [58]. Dimerization has also been studied in cell culture using bioluminescent complementation [59], native PAGE and cysteine crosslinking [60].

It was previously reported that ΔHD (Δ114-133) PrP^C, a deletion similar to that in ΔCR PrP^C, has a reduced dimerization propensity in N2a cells using native PAGE [60].

This group was also able to trap the dimer by adding a cysteine flanking the CR (S131C). We therefore used this latter strategy to study if ΔCR or G5 PrP^C would exhibit reduced dimerization. If the CR facilitates dimerization, then deleting it away (ΔCR PrP^C) or mutating it (G5 PrP^C) should result with reduced dimerization. This hypothesis was tested using S131C mutants of WT, ΔCR, G5, $G5_{\alpha1}$, and His to Ala PrP^C constructs.

The experimental protocol is schematized in Figure 5A. Briefly, if a cysteine on one PrP^C monomer is in close proximity and in the correct orientation to another cysteine, a disulfide can form. HEK293T cells were transfected with WT S131C PrP^C and then treated with phosphoinositide phospholipase C (PIPLC) to release PrP^C from the cell surface. Samples were then boiled in SDS buffer free of reducing agents and analyzed by western blot (Figure 5B). Blots were quantified by the percentage dimer band relative to total PrP^C in each lane (Figure 5C). In HEK293T cells, WT S131C PrP^C displayed an intense band corresponding to approximately 67 ± 4.6% dimer. However, the measured dimer band could be due to membrane crowding coupled to non-specific collisions between two PrP^C monomer's N-termini. To control for this possibility, a cysteine was added to the N-terminus (S36C) (Figure 5A). PIPLC-treated WT S36C PrP^C transfected cells analyzed by western blotting (Figure 5B) showed a very small band migrating as a dimer, and an extremely prominent monomer band. Therefore, the dimerization seen is specific for the CR.

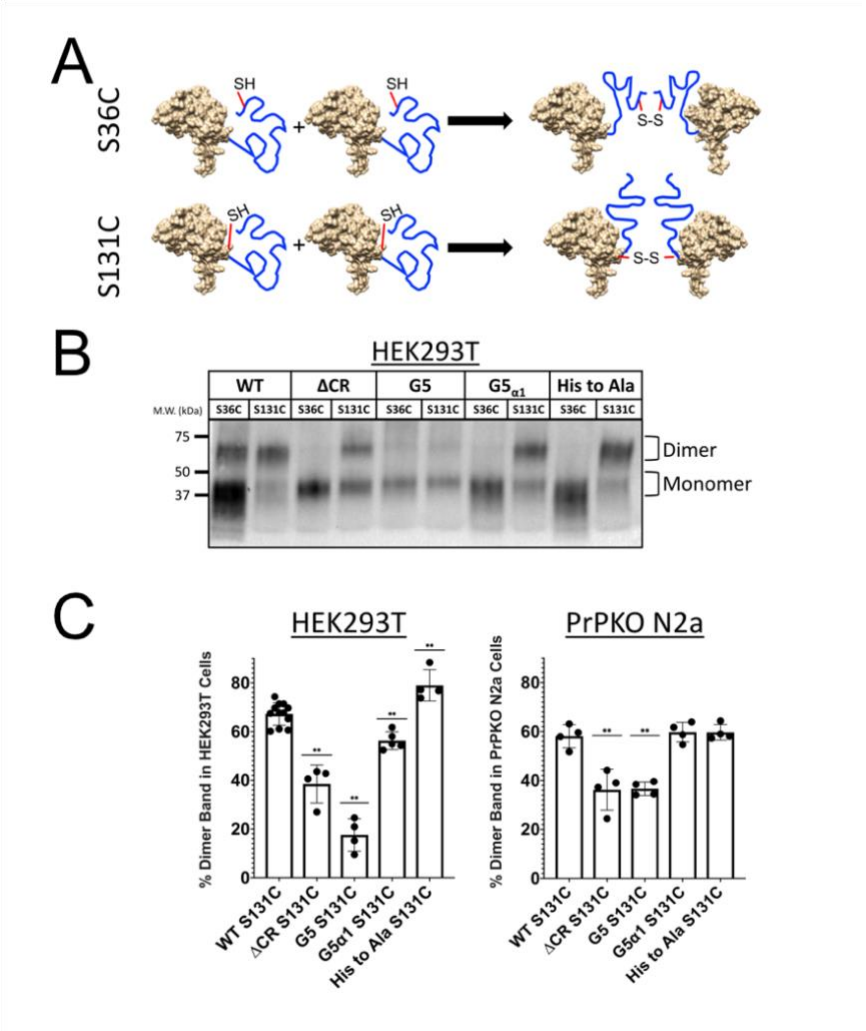

Figure 12: **ΔCR and G5 PrP^C have a reduced dimer band in cell surface cysteine crosslinking experiments at position S131C. A.** Schematic of the reaction occurring in the experiment. If two PrP^C molecules come close enough together in the right orientation, then disulfide formation will occur. Two separate positions were mutated (S36C and S131C). S36C was used to test if crosslinking only occurs due to cell surface crowding and S131C was used to test the specific interaction surface between two cell surface PrP^C molecules. **B.** Western blot of HEK293T cells transfected with one of the constructs either labeled at S36C or S131C. Samples were prepared by incubating cells with 0.1 U of PIPLC in PBS (+,+) for 2 hours rocking at 4 ^{o}C to remove only cell surface PrP^C. Samples were then boiled with SDS-PAGE gel loading buffer that did not contain reducing agent and loaded on to a SDS-PAGE gel. This allowed for the separation of a monomer and dimer band. When the constructs were labeled at S36C, there was little to no dimer band detectable. **C.** Quantitation of western blots for % Dimer band of samples labeled at S131C relative to the sum of monomer and dimer bands using densitometric analysis. Error bars represent ± S.D. for at least two different independent experiments. Asterisks denote significant differences when compared to WT S131C PrP^C (**P < 0.05). Results show that ΔCR, G5, and G5$_{\alpha1}$ PrP^C constructs have a reduced dimer band in HEK293T cells, where only ΔCR and G5 PrP^C have reduced dimer bands in PrPKO N2a cells.

Next, ΔCR, G5, $G5_{\alpha1}$, and His to Ala PrP^C (both S36C and S131C) constructs were tested (Figure 5B). For all constructs, similar to WT PrP^C, there was essentially no measurable dimer band for the S36C PrP^C mutants, however, dimer bands of varying intensity were observed for the S131C mutants. Compared to WT PrP^C, ΔCR S131C and G5 S131C PrP^C had a significantly reduced dimer bands of 39 ± 7.8% and 18 ± 6.6%, respectively. $G5_{\alpha1}$ S131C PrP^C resulted in a slightly reduced, but still significant, dimer band of 56 ± 3.7% when compared to WT PrP^C. Conversely, His to Ala S131C PrP^C had a slightly increased, but still significant, dimer band of 79 ± 6.4% percent relative to WT S131C PrP^C. These experiments were then repeated in PrPKO N2a cells (Figure 5C). Results were consistent with HEK293T cells, except that $G5_{\alpha1}$ S131C and His to Ala S131C PrP^C both had a comparable dimer band with WT PrP^C. Overall, the mutations to the CR led to the largest decrease in the measured dimer band. These suggest that the CR facilitates dimerization, an interaction that may play a role in regulation of the otherwise toxic N-terminal domain.

Addition of a cysteine in CR partially rescues toxicity

The addition of a cysteine just outside the CR (S131C) forces two PrP^C molecules to crosslink, as measured by western blot analysis (shown above). WT S131C PrP^C has a significantly larger dimer band when compared to ΔCR S131C and G5 S131C PrP^C constructs. However, there is still a dimer band for both ΔCR S131C and G5 S131C. This shows that the two constructs may still interact with an orientation

that allows for disulfide bond to formation, thereby forcing an irreversible dimer, albeit at a reduced level with respect to WT PrP^C.

The question then arises whether or not forcing dimerization in ΔCR S131C or G5 S131C PrP^C constructs rescues the cellular toxicity of these variants. To test this, a drug-based cellular assay (DBCA) was utilized [46]. Previously it was shown that ΔCR PrP^C expressing HEK293 cells have a lower cell viability when the media is supplemented with G418 for 48 hours. This is proposed to occur due to ΔCR PrP^C increasing drug influx by biasing cationic-selective membrane channels or by PrP^C directly forming cationic permeable pores through its N-terminus [61].

Therefore, transient transfections of PrP^C constructs in to HEK293T cells were performed and cell viability was assessed using WST-1. First, the non-cysteine constructs were tested (Figure 6A). Consistent with previous results, ΔCR PrP^C had a significant decrease in cell viability when compared to WT PrP^C. As expected, the other constructs with mutations in the CR (G5, $G5_{\alpha1,}$ and $G5_{\alpha23}$ PrP^C) also decreased in cell viability when compared to WT PrP^C. This is significant for $G5_{\alpha1}$ PrP^C because it is still undergoing cleavage in the cells, yet has a similar level of reduced cell viability as seen with ΔCR and G5 PrP^C.

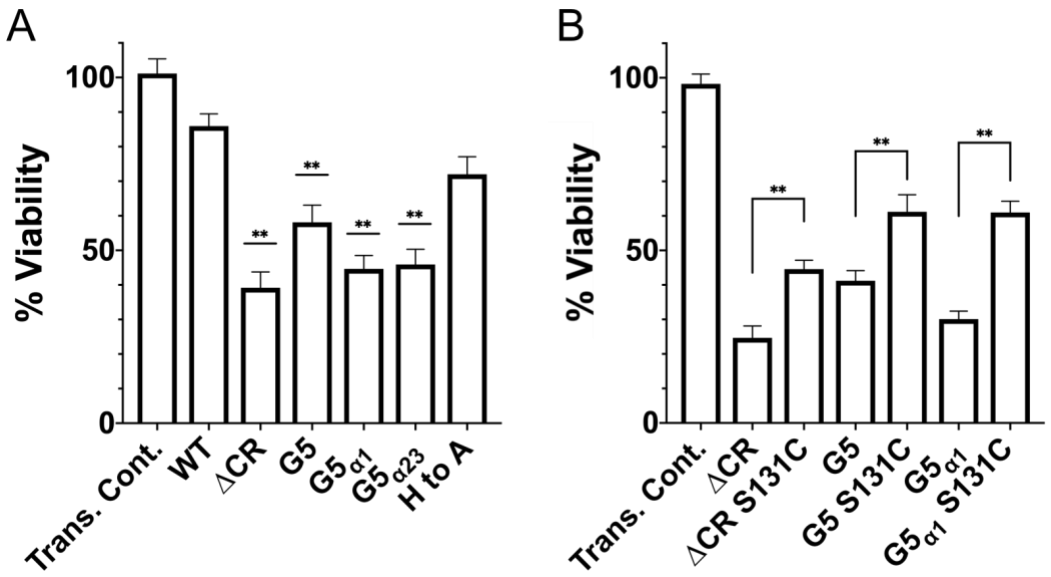

Figure 13: **Addition of a cysteine at position 131 partially regains cell viability**. **A)** HEK293T cells transfected with the indicated PrP^C construct were treated with 400 µg/mL G418 for 48 hours. Cell Viability was assessed by WST-1 reduction as described in the method section. Error bars represent ± S.E.M for at least three independent experiments. Asterisks denote significantly different when compared to WT (**P < 0.05). All mutants, except His to Ala PrP^C have a reduced cell viability relative to WT. **B.** Cysteine (S131C) constructs were tested with the non-cysteine construct to test if the reduction in cell viability could be increased. Asterisks denotes significantly different when compared to the particular PrP^C mutant without the added cysteine (**P < 0.05). ΔCR, G5, and $G5_{\alpha1}$ PrP^C constructs were able to be partially rescued by the addition of a cysteine.

To determine if the addition of a cysteine at position 131 can rescue the reduction in cell viability of PrP^C constructs with mutated CR, HEK293T cells were transfected with the cysteine-containing PrP^C constructs along with the non-cysteine containing constructs of ΔCR, G5, and $G5_{\alpha1}$ PrP^C (Figure 6B). For each cysteine-containing PrP^C construct, there was a partial, but still significant, increase in cell viability when compared to the non-cysteine PrP^C construct. This result demonstrates that forcing two PrP^C molecules together by the CR can decrease the toxicity elicited by the N-terminus.

Discussion

The molecular basis for the toxicity produced by elimination of the CR of PrP^C has remained unclear. Indeed, findings over the last two decades show, paradoxically, that the shorter the deletion, the more toxic the response [62, 63]. Here, we used protein design, NMR and electrophysiology to address this fundamental issue. Replacement of the CR region with a flexible linker of equivalent length recapitulates ΔCR PrP^C toxicity, as measured by spontaneous electrophysiological currents and toxicity induced by a DBCA. Reintroduction of consensus α-cleavage sites fails to dampen the observed currents. In addition, while it is now established that the WT CR segment supports the protective, metal ion-promoted *cis* N-terminal—C-terminal interaction, elimination of this interaction by replacement of OR His residues alone does not generate spontaneous currents or toxicity in the DBCA. Together, these results demonstrate that the spontaneous toxicity induced by deletion of the CR is not due exclusively to altering the length of the CR, blocking α-cleavage, or preventing the metal-driven *cis*-interaction. Rather, our results suggest that specific features of the CR sequence restrain the toxic activity of the PrP^C molecule, either by affecting the protein's interaction with itself or with other cell-surface molecules, or by altering the orientation of the N-terminal domain. Based on our recent structural and physiological studies of PrP^C, we propose three hypotheses, to explain how this might occur (Figure 7).

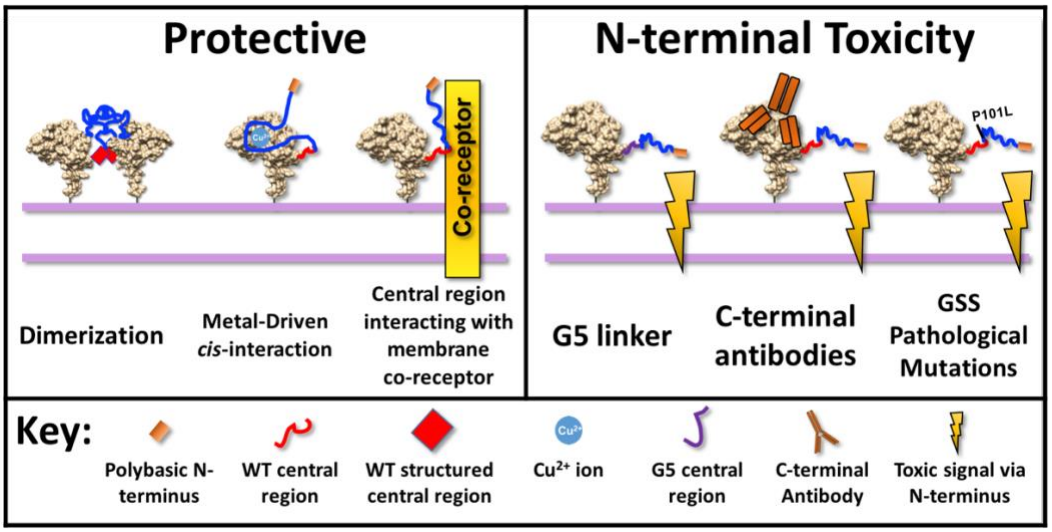

Figure 14: **N-terminal toxicity model.** WT PrP^C's CR sequence regulates the toxic effects of the extreme N-terminus. We hypothesize this can occur by three different mechanisms. First, the CR facilitates dimerization, which would move the extreme N-terminus away from causing toxicity. Second, Cu^{2+} binding allows the CR to reposition and hold the N-terminus away from generating toxicity. Third, the CR binds to a co-receptor which helps regulate the toxic potential of the N-terminus. When the CR is substituted with the G5 linker, or deleted in ΔCR PrP^C, the regulatory sequence of the CR is deleted and the N-terminus goes unregulated to cause toxic signaling. N-terminal toxicity can also possibly occur with C-terminal antibodies and CR pathological mutations causing GSS, such as P101L.

One hypothesis for the role of the CR is that it facilitates dimerization of PrP^C (Figure 7). Cellular cysteine crosslinking experiments show that WT PrP^C exhibits significantly greater dimerization than ΔCR and G5 PrP^C. This result demonstrates that a reduction in dimerization correlates with spontaneous currents and cell viability. Furthermore, enhancement of dimerization by introduction of the cysteine residues partially suppresses G418 induced toxicity relative to the non-cysteine versions of G5, ΔCR, and $G5_{\alpha1}$ PrP^C. A full restoration was likely not observed due to a large proportion of the constructs remaining in the monomeric form. Due to the incorporation of the non-native cysteine, we cannot be certain that the disulfide-stabilized dimer is physiological; however, our data suggests that the WT CR sequence enhances the

efficiency of two PrP^C molecules orienting correctly to allow for this disulfide bond to form. This agrees with a previous study that showed dimerization occurs at a specific interface [58].

How can dimerization regulate the toxic N-terminus? It is possible that homodimerization orients the otherwise toxic effector N-terminus in a way that prevents its misregulation. A previous study showed that C-terminal antibodies block dimerization as measured by bioluminescent complementation [59]. If the N-terminus is regulated by a PrP^C homodimer, then an antibody blocking dimerization would thus dislodge the N-terminus to elicit toxicity. This may explain why binding of C-terminal antibodies to WT PrP^C generates spontaneous currents [18]. Dimerization may also provide a mechanism by which overexpression of WT PrP^C rescues the toxicity of ΔCR PrP^C expressing cells. Specifically, an overabundance of WT PrP^C would force ΔCR PrP^C into a dimer, with cellular surface expression either *in cis* (same cell) [46] or *in trans* (adjacent cells) [44], thus regulating ΔCR PrP^C's toxic N-terminus.

Our data are also consistent with a model in which the CR of PrP^C forces the N-terminus to orient away from the membrane when engaged in the metal-driven *cis*-interaction (Figure 7). This orientation, which would depend on specific sequence characteristics of the CR, would be absent in ΔCR and G5 PrP^C, thus liberating the N-terminus to generate a toxic signal. This proposal agrees with a molecular model generated using restraints from NMR and mass spectrometry crosslinking experiments [22].

A third plausible model posits that the CR docks to an unknown co-membrane receptor (Figure 7). This model is consistent with data describing PrP^C as a regulator of both ionotropic [14, 64] and metabotropic [65, 66] glutamatergic receptors. Additionally, ΔCR PrP^C expressing cells are sensitive to glutamate induced excitotoxicity [45]. However, ΔCR PrP^C induced currents occur in both mammalian and insect cells [41], which possess very different complements of membrane receptors, suggesting that spontaneous currents originate from intrinsic PrP^C properties, and not by misregulation of a membrane co-receptor.

Our findings may provide insight into the distinct phenotypes of inherited prion disease. Familial prion diseases are caused by mutations in two main regions. The first region is near the conserved negatively charged patch on the C-terminus (e.g. D177N and E199K) [19], mutations in which typically cause CJD or fatal familial insomnia [67]. The second region encompasses the CR (e.g. P101L and A116V), mutations in which typically cause GSS. Both CJD mutations (D177N and E199K), as well as GSS mutations (P101L and A116V) have a near 100% penetrance [68]. Several lines of evidence show, however, that there are substantial phenotypic differences between the two sets of disease-causing mutations. These include differences in plaque conformation [27, 69-71], generation of spontaneous currents and G418 induced toxicity, [43], and metal-driven *cis*-interaction [19, 22]. These observations suggest that mutations in the two regions act via different pathological mechanisms. Given that only CR mutations cause spontaneous currents, G418 induced toxicity, and

a WT PrP^C-like *cis*-interaction, it is possible that the toxic mechanisms of CR GSS causing mutations originate from an N-terminal toxicity model, similar to ΔCR PrP^C, G5 PrP^C and C-terminal antibodies (Figure 7). This can be due to reduction in dimerization or modulation of the conformational landscape of the CR. Conversely, C-terminal CJD causing mutations may produce toxicity by other mechanisms, for example by enhancing aggregation of the protein or otherwise altering its biochemical properties.

In summary, our results demonstrate that the CR is not a passive linker connecting the N- and C-terminal domains. Instead, specific features of the sequence are absolutely crucial for blocking toxicity generated by the otherwise unregulated N-terminus. We propose that the CR either facilitates homodimerization of PrP^C or serves to conformationally restrict the N-terminus from driving toxicity. Further elucidation of these regulatory contacts will be important for advancing concepts of prion toxicity.

References

1. Prusiner, S.B., *Novel proteinaceous infectious particles cause scrapie.* Science, 1982. **216**(4542): p. 136-44.
2. Collinge, J., *Prion diseases of humans and animals: their causes and molecular basis.* Annu Rev Neurosci, 2001. **24**: p. 519-50.
3. Brandner, S., et al., *Normal host prion protein necessary for scrapie-induced neurotoxicity.* Nature, 1996. **379**(6563): p. 339-43.

4. Watt, N.T., H.H. Griffiths, and N.M. Hooper, *Lipid rafts: linking prion protein to zinc transport and amyloid-beta toxicity in Alzheimer's disease.* Front Cell Dev Biol, 2014. **2**: p. 41.

5. Barmada, S., et al., *GFP-tagged prion protein is correctly localized and functionally active in the brains of transgenic mice.* Neurobiol Dis, 2004. **16**(3): p. 527-37.

6. Peralta, O.A. and W.H. Eyestone, *Quantitative and qualitative analysis of cellular prion protein (PrP(C)) expression in bovine somatic tissues.* Prion, 2009. **3**(3): p. 161-70.

7. Sales, N., et al., *Cellular prion protein localization in rodent and primate brain.* Eur J Neurosci, 1998. **10**(7): p. 2464-71.

8. Hornemann, S., et al., *Recombinant full-length murine prion protein, mPrP(23-231): purification and spectroscopic characterization.* FEBS Letters, 1997. **413**(2): p. 277-281.

9. Aronoff-Spencer, E., et al., *Identification of the Cu2+ binding sites in the N-terminal domain of the prion protein by EPR and CD spectroscopy.* Biochemistry, 2000. **39**(45): p. 13760-71.

10. Burns, C.S., et al., *Copper coordination in the full-length, recombinant prion protein.* Biochemistry, 2003. **42**(22): p. 6794-803.

11. Chattopadhyay, M., et al., *The octarepeat domain of the prion protein binds Cu(II) with three distinct coordination modes at pH 7.4.* J Am Chem Soc, 2005. **127**(36): p. 12647-56.

12. Millhauser, G.L., *Copper and the prion protein: methods, structures, function, and disease.* Annu Rev Phys Chem, 2007. **58**: p. 299-320.

13. Walter, E.D., et al., *The prion protein is a combined zinc and copper binding protein: Zn2+ alters the distribution of Cu2+ coordination modes.* J Am Chem Soc, 2007. **129**(50): p. 15440-1.

14. Watt, N.T., et al., *Prion protein facilitates uptake of zinc into neuronal cells.* Nat Commun, 2012. **3**: p. 1134.

15. You, H., et al., *Abeta neurotoxicity depends on interactions between copper ions, prion protein, and N-methyl-D-aspartate receptors.* Proc Natl Acad Sci U S A, 2012. **109**(5): p. 1737-42.

16. Pushie, M.J., et al., *Prion protein expression level alters regional copper, iron and zinc content in the mouse brain.* Metallomics, 2011. **3**(2): p. 206-14.

17. Evans, E.G.B. and G.L. Millhauser, *Copper- and Zinc-Promoted Interdomain Structure in the Prion Protein: A Mechanism for Autoinhibition of the Neurotoxic N-Terminus.* Prog Mol Biol Transl Sci, 2017. **150**: p. 35-56.

18. Wu, B., et al., *The N-terminus of the prion protein is a toxic effector regulated by the C-terminus.* Elife, 2017. **6**.

19. Spevacek, A.R., et al., *Zinc drives a tertiary fold in the prion protein with familial disease mutation sites at the interface.* Structure, 2013. **21**(2): p. 236-46.

20. Evans, E.G., et al., *Interaction between Prion Protein's Copper-Bound Octarepeat Domain and a Charged C-Terminal Pocket Suggests a Mechanism for N-Terminal Regulation.* Structure, 2016. **24**(7): p. 1057-67.

21. Thakur, A.K., et al., *Copper alters aggregation behavior of prion protein and induces novel interactions between its N- and C-terminal regions.* J Biol Chem, 2011. **286**(44): p. 38533-45.

22. McDonald, A.J., et al., *Altered Domain Structure of the Prion Protein Caused by Cu(2+) Binding and Functionally Relevant Mutations: Analysis by Cross-Linking, MS/MS, and NMR.* Structure, 2019. **27**(6): p. 907-922 e5.

23. Martinez, J., et al., *PrP charge structure encodes interdomain interactions.* Sci Rep, 2015. **5**: p. 13623.

24. Markham, K.A., et al., *Molecular Features of the Zn(2+) Binding Site in the Prion Protein Probed by (113)Cd NMR.* Biophys J, 2019. **116**(4): p. 610-620.

25. Sonati, T., et al., *The toxicity of antiprion antibodies is mediated by the flexible tail of the prion protein.* Nature, 2013. **501**(7465): p. 102-6.

26. Herrmann, U.S., et al., *Prion infections and anti-PrP antibodies trigger converging neurotoxic pathways.* PLoS Pathog, 2015. **11**(2): p. e1004662.

27. Coleman, B.M., et al., *Pathogenic mutations within the hydrophobic domain of the prion protein lead to the formation of protease-sensitive prion species with increased lethality.* J Virol, 2014. **88**(5): p. 2690-703.

28. Schatzl, H.M., et al., *Prion protein gene variation among primates.* J Mol Biol, 1995. **245**(4): p. 362-74.

29. Liang, J. and Q. Kong, *alpha-Cleavage of cellular prion protein.* Prion, 2012. **6**(5): p. 453-60.

30. McDonald, A.J., et al., *A new paradigm for enzymatic control of alpha-cleavage and beta-cleavage of the prion protein.* J Biol Chem, 2014. **289**(2): p. 803-13.

31. Kuffer, A., et al., *The prion protein is an agonistic ligand of the G protein-coupled receptor Adgrg6.* Nature, 2016. **536**(7617): p. 464-8.

32. Westergard, L., J.A. Turnbaugh, and D.A. Harris, *A naturally occurring C-terminal fragment of the prion protein (PrP) delays disease and acts as a dominant-negative inhibitor of PrPSc formation.* J Biol Chem, 2011. **286**(51): p. 44234-42.

33. Chen, S., S.P. Yadav, and W.K. Surewicz, *Interaction between human prion protein and amyloid-beta (Abeta) oligomers: role OF N-terminal residues.* J Biol Chem, 2010. **285**(34): p. 26377-83.

34. Lauren, J., et al., *Cellular prion protein mediates impairment of synaptic plasticity by amyloid-beta oligomers.* Nature, 2009. **457**(7233): p. 1128-32.

35. Shmerling, D., et al., *Expression of amino-terminally truncated PrP in the mouse leading to ataxia and specific cerebellar lesions.* Cell, 1998. **93**(2): p. 203-14.

36. Baumann, F., et al., *Lethal recessive myelin toxicity of prion protein lacking its central domain.* EMBO J, 2007. **26**(2): p. 538-47.

37. Christensen, H.M., et al., *A highly toxic cellular prion protein induces a novel, nonapoptotic form of neuronal death.* Am J Pathol, 2010. **176**(6): p. 2695-706.

38. Li, A., et al., *Neonatal lethality in transgenic mice expressing prion protein with a deletion of residues 105-125.* EMBO J, 2007. **26**(2): p. 548-58.

39. Westergard, L., H.M. Christensen, and D.A. Harris, *The cellular prion protein (PrP(C)): its physiological function and role in disease.* Biochim Biophys Acta, 2007. **1772**(6): p. 629-44.

40. Christensen, H.M. and D.A. Harris, *A deleted prion protein that is neurotoxic in vivo is localized normally in cultured cells.* J Neurochem, 2009. **108**(1): p. 44-56.

41. Solomon, I.H., J.E. Huettner, and D.A. Harris, *Neurotoxic mutants of the prion protein induce spontaneous ionic currents in cultured cells.* J Biol Chem, 2010. **285**(34): p. 26719-26.

42. Massignan, T., E. Biasini, and D.A. Harris, *A Drug-Based Cellular Assay (DBCA) for studying cytotoxic and cytoprotective activities of the prion protein: A practical guide.* Methods, 2011. **53**(3): p. 214-9.

43. Solomon, I.H., et al., *An N-terminal polybasic domain and cell surface localization are required for mutant prion protein toxicity.* J Biol Chem, 2011. **286**(16): p. 14724-36.

44. Biasini, E., et al., *The toxicity of a mutant prion protein is cell-autonomous, and can be suppressed by wild-type prion protein on adjacent cells.* PLoS One, 2012. **7**(3): p. e33472.

45. Biasini, E., et al., *A mutant prion protein sensitizes neurons to glutamate-induced excitotoxicity.* J Neurosci, 2013. **33**(6): p. 2408-18.

46. Massignan, T., et al., *A novel, drug-based, cellular assay for the activity of neurotoxic mutants of the prion protein.* J Biol Chem, 2010. **285**(10): p. 7752-65.

47. Westergard, L., J.A. Turnbaugh, and D.A. Harris, *A nine amino acid domain is essential for mutant prion protein toxicity.* J Neurosci, 2011. **31**(39): p. 14005-17.

48. McDonald, A.J., B. Wu, and D.A. Harris, *An inter-domain regulatory mechanism controls toxic activities of PrP(C).* Prion, 2017. **11**(6): p. 388-397.

49. Turnbaugh, J.A., et al., *The N-terminal, polybasic region is critical for prion protein neuroprotective activity.* PLoS One, 2011. **6**(9): p. e25675.

50. Gibson, D.G., et al., *Enzymatic assembly of DNA molecules up to several hundred kilobases.* Nat Methods, 2009. **6**(5): p. 343-5.

51. Mehrabian, M., et al., *CRISPR-Cas9-based knockout of the prion protein and its effect on the proteome.* PLoS One, 2014. **9**(12): p. e114594.

52. Delaglio, F., et al., *NMRPipe: a multidimensional spectral processing system based on UNIX pipes.* J Biomol NMR, 1995. **6**(3): p. 277-93.

53. Pettersen, E.F., et al., *UCSF Chimera--a visualization system for exploratory research and analysis.* J Comput Chem, 2004. **25**(13): p. 1605-12.

54. Oliveira-Martins, J.B., et al., *Unexpected tolerance of alpha-cleavage of the prion protein to sequence variations.* PLoS One, 2010. **5**(2): p. e9107.

55. Chen, X., J.L. Zaro, and W.C. Shen, *Fusion protein linkers: property, design and functionality.* Adv Drug Deliv Rev, 2013. **65**(10): p. 1357-69.

56. Liang, J., et al., *Cellular prion protein regulates its own alpha-cleavage through ADAM8 in skeletal muscle.* J Biol Chem, 2012. **287**(20): p. 16510-20.

57. Fioriti, L., et al., *The neurotoxicity of prion protein (PrP) peptide 106-126 is independent of the expression level of PrP and is not mediated by abnormal PrP species.* Mol Cell Neurosci, 2005. **28**(1): p. 165-76.

58. Sangeetham, S.B., et al., *Interrogating the Dimerization Interface of the Prion Protein Via Site-Specific Mutations to p-Benzoyl-L-Phenylalanine.* J Mol Biol, 2018. **430**(17): p. 2784-2801.

59. Wusten, K.A., et al., *A Bioluminescent Cell Assay to Quantify Prion Protein Dimerization.* Sci Rep, 2018. **8**(1): p. 14178.

60. Rambold, A.S., et al., *Stress-protective signalling of prion protein is corrupted by scrapie prions.* EMBO J, 2008. **27**(14): p. 1974-84.

61. Solomon, I.H., E. Biasini, and D.A. Harris, *Ion channels induced by the prion protein: mediators of neurotoxicity.* Prion, 2012. **6**(1): p. 40-5.

62. McDonald, A.J. and G.L. Millhauser, *PrP overdrive: does inhibition of alpha-cleavage contribute to PrP(C) toxicity and prion disease?* Prion, 2014. **8**(2).

63. Yusa, S., et al., *Cellular prion protein: from physiology to pathology.* Viruses, 2012. **4**(11): p. 3109-31.

64. Stys, P.K., H. You, and G.W. Zamponi, *Copper-dependent regulation of NMDA receptors by cellular prion protein: implications for neurodegenerative disorders.* J Physiol, 2012. **590**(6): p. 1357-68.

65. Goniotaki, D., et al., *Inhibition of group-I metabotropic glutamate receptors protects against prion toxicity.* PLoS Pathog, 2017. **13**(11): p. e1006733.

66. Um, J.W., et al., *Metabotropic glutamate receptor 5 is a coreceptor for Alzheimer abeta oligomer bound to cellular prion protein.* Neuron, 2013. **79**(5): p. 887-902.

67. Aguzzi, A., F. Baumann, and J. Bremer, *The prion's elusive reason for being.* Annu Rev Neurosci, 2008. **31**: p. 439-77.

68. Minikel, E.V., et al., *Quantifying prion disease penetrance using large population control cohorts.* Sci Transl Med, 2016. **8**(322): p. 322ra9.

69. Collins, S., C.A. McLean, and C.L. Masters, *Gerstmann-Straussler-Scheinker syndrome,fatal familial insomnia, and kuru: a review of these less common human transmissible spongiform encephalopathies.* J Clin Neurosci, 2001. **8**(5): p. 387-97.

70. Kitamoto, T., et al., *Amyloid plaques in Creutzfeldt-Jakob disease stain with prion protein antibodies.* Ann Neurol, 1986. **20**(2): p. 204-8.

71. Masters, C.L., D.C. Gajdusek, and C.J. Gibbs, Jr., *Creutzfeldt-Jakob disease virus isolations from the Gerstmann-Straussler syndrome with an analysis of the various forms of amyloid plaque deposition in the virus-induced spongiform encephalopathies.* Brain, 1981. **104**(3): p. 559-88.

CHAPTER 3

Central Region Pathological Mutations Do Not Affect the Copper-Driven *cis*-Interaction

Introduction

Prion diseases are a class of neurodegenerative disorders called transmissible spongiform encephalopathies (TSE). These diseases are caused by the misfolding of the cellular prion protein (PrP^{C}) into the toxic and aggregation prone conformer (PrP^{Sc}) [1, 2]. The misfolded PrP^{Sc} seed will subsequently dock to additional PrP^{C} and drive a template-directed misfolding event to produce more PrP^{Sc}. Postmortem analyses of brains affected by prion diseases show massive neurodegeneration and spongiform in addition to different types amyloid deposits, depending on the disease. These disorders occur in humans and include the diseases Creutzfeldt-Jakob Disease (CJD), Gerstmann–Sträussler–Scheinker syndrome (GSS), and Kuru [3]. CJD can be caused by the spontaneous misfolding of PrP^{C} as well as by pathological mutations in the protein, but GSS is only caused by pathological mutations. In contrast, Kuru affected the South Fore people in Papua New Guinea and was spread by ritualistic cannibalism. These diseases also affect animals such as Scrapie in sheep and Bovine Spongiform Encephalopathies in cattle.

Despite understanding the propagation mechanism of prion diseases, the exact biological function of PrP^{C} is unknown or whether the disease state is due to a loss of function, a gain of function, or exacerbation of PrP^{C} native function. PrP^{C} is composed of an unstructured N-terminus and a globular C-terminal domain. These domains are connected by a highly-conserved central region. The C-terminal domain is composed of three α-helices, one short anti-parallel ß-sheet, and a highly conserved

negatively-charged surface patch. Posttranslational modifications of the C-terminal domain include formation of a disulfide bond between helices two and three, two glycosylation sites, and a glycosylphosphatidylinositol (GPI) anchor at the C-terminal end of PrP^C that anchors the protein to the outer leaflet of neurons. The unstructured N-terminus includes a polybasic extreme N-terminus and the octarepeat (OR) domain. The OR binds to metal ions, specifically having an affinity for Cu^{2+} and Zn^{2+} at physiologically relevant concentrations [4]. In particular, Cu^{2+} binds to the OR, depending on the metal ion concentration and pH. Due the metal binding properties, PrP^C's function has been proposed to be metal-ion dependent. These functions include, but are not limited to, neuroprotective function, ion-channel regulation, and metal ion localization.

Most structural analysis of PrP^C has been done on either the isolated C-terminal or N-terminal domain, because it was believed that they do not interact. However, recent evidence shows that they do interact, and the interaction is facilitated by one equivalent of Cu^{2+} or Zn^{2+} binding to the OR [5-8]. Upon the OR binding to one equivalent of either Zn^{2+} or Cu^{2+}, the N-terminus becomes slightly structured and docks to a highly-conserved negatively charged patch on the C-terminus. This docking event is called the metal-driven *cis*-interaction.

This interaction is of interest due to observed toxicity generated by antibodies that bind to the C-terminus of PrP^C [9]. The epitope of these toxic C-terminal antibodies overlaps with the surface where the *cis*-interaction occurs. Furthermore,

the toxicity generated by C-terminal antibodies is similar to that observed for prion diseases [10] without the need for protein misfolding. C-terminal antibody-induced toxicity is blocked by the addition of antibodies directed to the N-terminus of PrP^C as well as by the deletion of the extreme N-terminus. Overall, this leads to a model in which the polybasic extreme N-terminus has an inherent toxic or effector function and the globular C-terminus regulates it by allowing for the metal-driven *cis*-interaction [7]. When the N-terminus is then released, by antibodies or various mutations, the N-terminus can cause toxicity, which is called the N-terminal toxicity model.

It was recognized that mutations on the C-terminus that cause genetic prion diseases affect the conserved negatively-charged patch, which is known to be important for the metal-driven *cis*-interaction [8]. It was shown that these pathological mutations alter the Zn^{2+} and Cu^{2+}-driven *cis*-interaction [8, 11]. Interestingly, these mutations typically cause CJD. Another region where there is a high density of pathological mutations is the central region of PrP^C. These mutations typically cause GSS. One of these mutations, P101L, was shown to have a slightly weakened Zn^{2+}-driven interaction. We hypothesized that the C-terminal and central region pathological mutations have a similar weakening of the metal-driven *cis*-interaction.

This study uses NMR to test if central region pathological mutations have a weakened Cu^{2+}-driven *cis*-interaction. The results of this study show, both

qualitatively and quantitatively, that there is no difference in the Cu^{2+}-driven *cis*-interaction between WT PrP^C and the central region pathological mutants tested. These results suggest that there is a possible difference in toxicity between central region pathological mutations, which cause GSS, and C-terminal pathological mutations, which cause CJD.

Materials and Methods

Protein Expression

Recombinant PrP constructs encoding mouse WT PrP^C (23-230) and the various central region pathological mutants constructs in the pJ414 vector (DNA 2.0) were transformed into and expressed using *E. coli* (BL21 (DE3) Invitrogen) [5].

Bacteria were grown in M9 minimal media supplemented with $^{15}NH_4Cl$ (1 g/L) (Cambridge Isotopes) for ^{1}H-^{15}N HSQC experiments or in LB media (Research Product International). Cells were grown at 37°C until reaching an optical density (OD) of 1-1.2, at which point expression was induced with 1 mM isopropyl-1-thio-D-galactopyranoside (IPTG). PrP^C constructs were purified as previously described [8]. Briefly, proteins were extracted from inclusion bodies with extraction buffer (8 M guanidium chloride (GdnHCl), 100 mM Tris, 100 mM Sodium Acetate (pH 8)) at room temperature and were purified by Ni^{2+}-immobilized metal-ion chromatography (IMAC). Proteins were eluted from the IMAC column using elution butter (5 M GdnHCl, 100 mM Tris, 100 mM Sodium Acetate (pH 4.5)) and were brought to pH 8 with 6 M

potassium hydroxide (KOH) and left at 4°C for 2 days to oxidize the native disulfide bond. Proteins were then desalted into 50 mM potassium acetate buffer (pH 4.5) and purified by reverse-phase HPLC on a C_4 column (Grace). Pure protein was lyophilized and stored at -20 ^oC until needed. The purity and identity of all constructs were verified by analytical HPLC and mass spectrometry (ESI-MS).

NMR

Lyophilized uniformly ^{15}N-labeled PrP^C constructs were first suspended in water until fully solubilized and concentrations were checked using absorbance at 280 nm (A_{280}) with the proper extinction coefficient. NMR samples were made to 300 µM in 10 mM 2-(*N*-morpholino)ethanesulfonic acid (MES) buffer with 10% D_2O and the pH was adjusted to 6.1 with 600 mM hydrochloric acid. Apo samples were loaded into a Shigemi NMR tube (Wilmad Glass, BMS-005B) and a ^1H- ^{15}N HSQC spectrum as collected at 37 ^oC on an 800-MHz spectrometer (Bruker, Billerica, MA) at the University of California, Santa Cruz NMR Facility (Santa Cruz, CA). The sample was then removed from the tube and one equivalent of Cu^{2+} from a 10 mM copper chloride solution in water (determined accurately by flame atomic absorption) was added and the pH was adjusted to 6.1 if necessary. The sample was loaded back into the Shigemi NMR tube and the sample height was adjusted to match the sample height of the apo sample and another ^1H- ^{15}N HSQC spectrum was collected. NMR spectra were analyzed with NMRPipe [12] and Sparky. Structural analysis was performed with

Chimera [13]. Protein assignments were achieved using previously determined values [5]. Kernel density estimation were performed in MATLAB. To eliminate the effects of differential nonspecific broadening across mutants, the data was adjusted so that the center of the unaffected peak for each PrP construct were aligned to 1.

Results

Multiple disease-causing mutations occur around the central region of PrP^C, which include: P101L, P104L, P104T, G113V, A116V, and G130V (Figure 1). In particular, P101L, G113V, and to a weaker extent A116V PrP^C, display spontaneous currents in cellular electrophysiological measurements and G418 induced toxicity in cells [14]. It has been previously shown that C-terminal pathological mutations affect both the Zn^{2+} [8] and Cu^{2+}-driven *cis*-interaction [7, 15]. One central region pathological mutation, P101L PrP^C, was shown to have a slightly weakened Zn^{2+}-driven *cis*-interaction. Therefore, we hypothesize that these central region pathological mutations might weaken the Cu^{2+}-driven *cis*-interaction, thus freeing up the N-terminus to cause toxicity, according to the N-terminal toxicity model [16]. Alternatively, these mutations may not affect the Cu^{2+}-driven *cis*-interaction, implying an alternative mechanism of toxicity.

Construct	Disease Type	Currents	G418 Toxicity
WT	None	–	–
P101L	GSS (129M)	+	+
P104L	GSS (129V)	–	–
P104T	Atypical Prion Disease	–	–
G113V	Familial Dementia	+	+
A116V	GSS (129V)	–	–

Figure 15: **Central region disease causing mutations.** Some of these mutations generate spontaneous currents in electrophysiological measurements as well G418 induced toxicity.

To investigate if the central region pathological mutations have a weakened Cu^{2+}-driven *cis*-interaction, paramagnetic relaxation enhancement NMR was employed [5] as described in chapter 2 of this dissertation. Uniformly ^{15}N-labeled protein was prepared for each construct and ^{1}H-^{15}N HSQC spectra were collected in the absence and presence of 1 eq. of Cu^{2+}. The intensity of the resonance with 1 eq. of Cu^{2+} (I) was divided by the intensity of the resonance in the absence of Cu^{2+} (I_o) to generate intensity ratios (I/I_o). I/I_o vs. residue plots were made for all the pathological mutations (Figure 2). At initial investigation, all of the bar graphs appear similar and implies a similar Cu^{2+}-driven *cis*-interaction for each pathological mutation as compared to WT PrP^C.

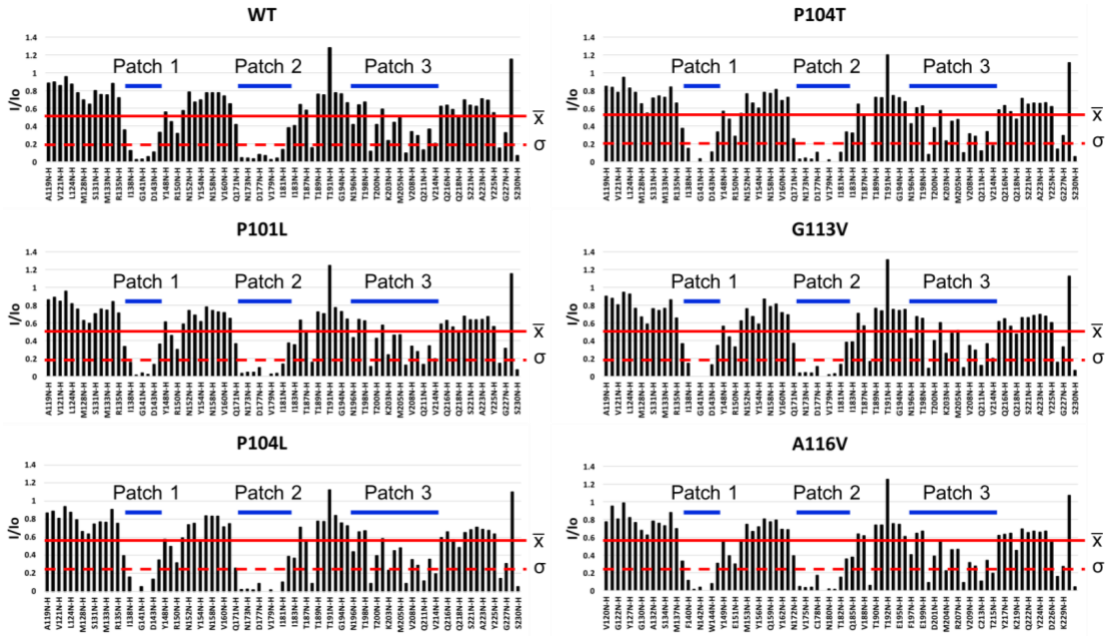

Figure 16: **Normalized NMR intensity plots of CR pathological mutations**. I/Io vs. residues plot of WT, P101L, P104L, P104T, G113V, and A116V PrP^C constructs titrated with 1 eq. of Cu^{2+} at pH 6.1 and 37 °C. The averages ($\bar{x}$) and standard deviation (σ) of only similar residues of each construct were taken. The plots show little difference between central region pathological mutations relative to WT PrP^C in Cu^{2+} titration.

The I/I_o were then transformed into kernel density distributions [7] (Figure 3). This was done to gain an unbiased measure of the relative number of C-terminal residues affected by the Cu^{2+}-driven *cis*-interaction. To do this, the I/I_o values were normalized so the residues unaffected have an adjusted I/I_o equal to about 1 as described in the methods section. The kernel density function was then used on the adjusted I/I_o values for each construct to generate kernel density estimation plots (Figure 3). The plots show adjusted I/I_o vs. probability of having that I/I_o value. Two main populations arose, one centered at about one corresponding to the residues not affected and the other centered around 0.2 corresponding to residues affected. Overall the overlaid kernel density estimations appear similar for WT PrP^C when

compared to the central region pathological mutations. This is in good agreement with the visual inspection of the raw I/I_o values.

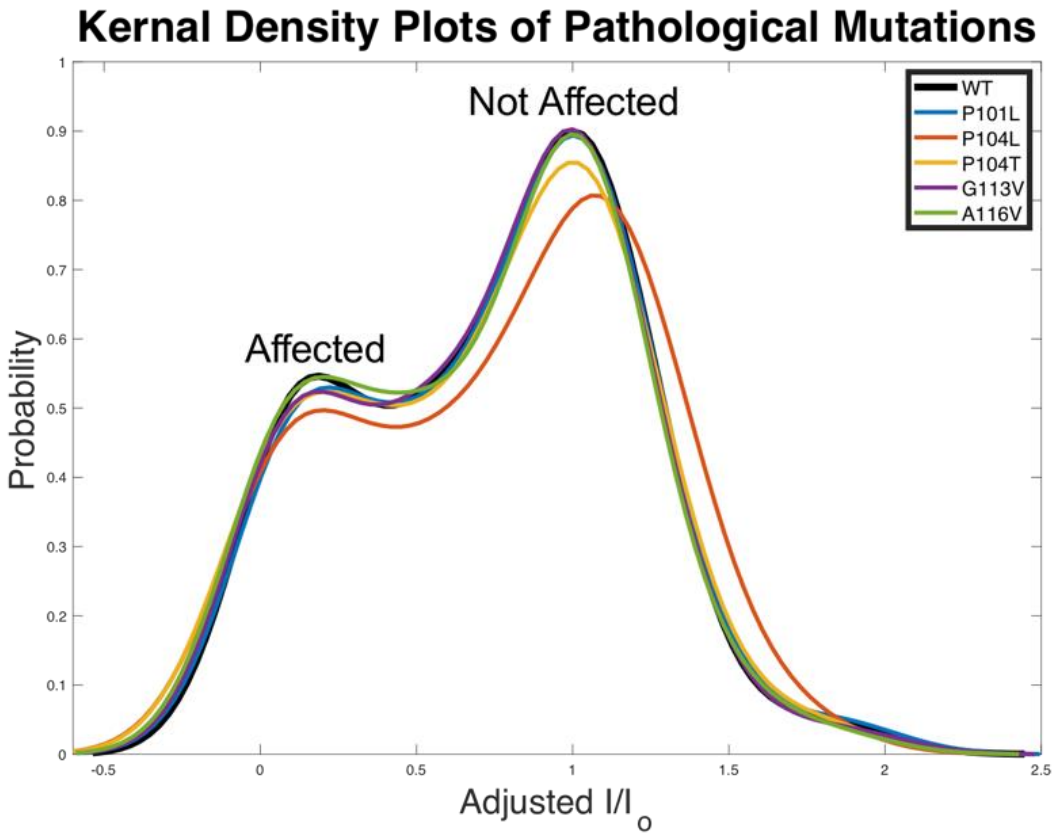

Figure 17: **Kernel density distributions of CR pathological mutations.** The distributions show little difference between the number of affected residues between central region pathological mutations relative to WT PrP^C. Kernel density distributions of the I/I_o values for each protein were generated by calculated by applying a gaussian-weighted sliding window. I/I_o values were initially adjusted by first generating a kernel density distribution for each construct and the 'Not Affected' peak was set to about 1.

To define which residues are significantly affected, the average ($\bar{x}$) and standard deviation (σ) of the raw I/I_o values of each construct were taken (Figure 2). Residues considered strongly affected by the addition of Cu^{2+} are those residues affected by greater than one standard deviation (1σ). For each construct, the residues affected by greater than 1σ are the same and they are highlighted in blue on the

surface representation of the PrP^C C-terminal domain (PDB: 1XYX) (Figure 4). The affected residues are localized to three main patches (Figure 2 and 4): the C-terminal end of the loop going into helix 1 (Patch 1), the N-terminal end of helix 2 (Patch 2), and the N-terminal half of helix 3 (Patch 3). These results qualitatively demonstrate that the central region pathological mutations do not affect the Cu^{2+}-driven *cis*-interaction.

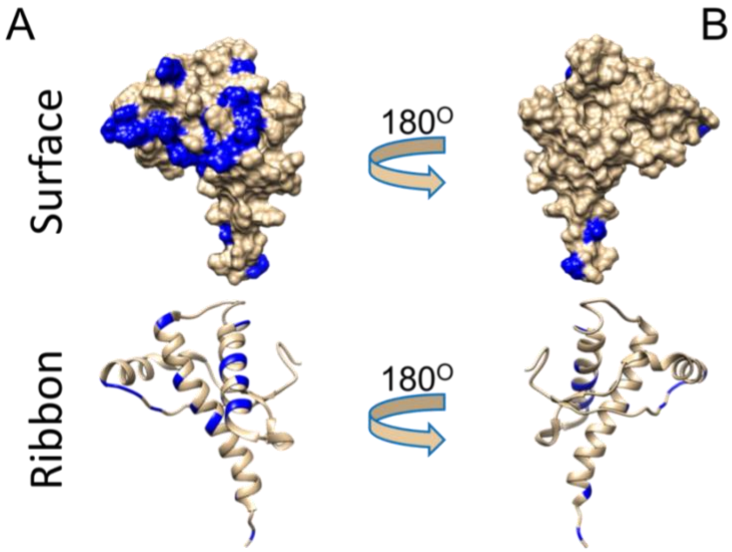

Patch 1	Patch 2	Patch 3
I138	N172	E199
F140	N173	R207
G141	V175	Q211
N142	D177N	V214
D143	C178	D226*
	V179	S230*
	N180	
	I181	
	V188*	

Figure 18: **Cu^{2+} affects the same C-terminal residues for CR pathological mutations and WT PrP^C. A.** Surface representation (top) and ribbon diagram (bottom) of the C-terminus of PrP^C (PDB: 1XYX). Residues in blue are the residues where the I/I_o values are affected by greater than 1σ by the addition of 1 eq. of Cu^{2+}. The residues affected by 1σ for the central region mutations and WT PrP^C are the same. **B.** Table of residues affected by 1σ classified by patch. Patch 1 is the loop going into helix 1. Patch 2 in the N-terminal side of helix 2. Patch 3 is the N-terminal end of helix 3. Asterisks denote residues affected near particular patch.

To be quantitate the *cis*-interaction, the average I/I_o of each patch was taken. This is similar to the quantitative method done previously [8], in which the average I/I_o of each helix was taken and compared for different constructs. Due to the localization of Patch 1 residing on the loop going into helix 1, the average of each

patch plus one residue on each side was taken and plotted as a bar graph (Figure 5). Similar to the residues being affected by greater than 1σ, all central region pathological mutants were within error of the patch averages for WT PrP^C. For Patch 2, there seems to be a small decrease in patch average for P104L and P104T PrP^C, however, this is within error when compared to WT PrP^C. Overall, this analysis shows that the regions where Cu^{2+} affects is the same for all of the central region pathological mutations as compared to WT PrP^C.

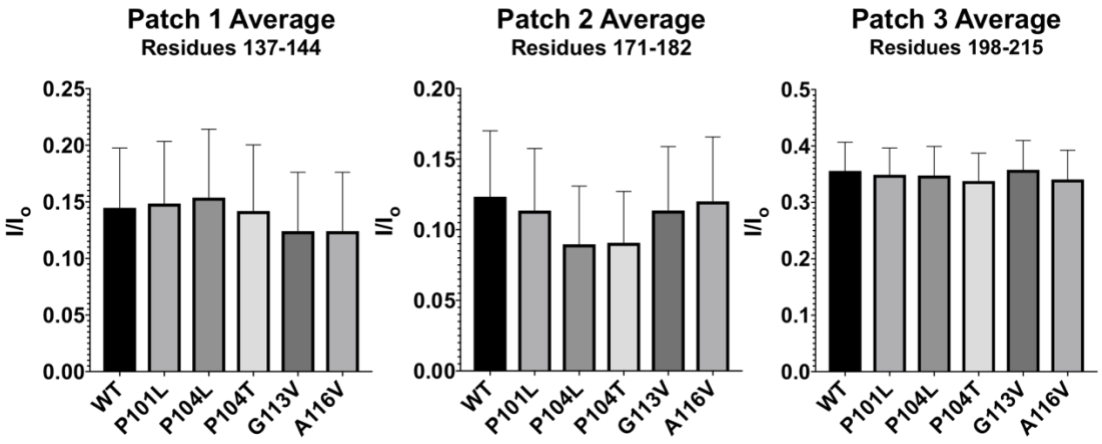

Figure 19: **Average I/I_o values for each defined patch is the same for CR pathological mutations and WT PrP^C.** Bar graphs of the average I/I_o values for each patch are shown. Error bars denote the standard error of the mean (S.E.M). For each patch there is no statistical difference in average I/I_o values for the central region pathological mutations when compared to WT PrP^C. For Patch 2, it P104L and P104T have a slightly lower than everything, however, it is not statistically significant.

Discussion

Due to the rich literature pertaining to PrP^C binding to metal ions in the OR domain, specifically Zn^{2+} and Cu^{2+}, PrP^C's function is suggested to be related to its metal binding properties. These functions include, but are not limited to, neuroprotective effects as a result of oxidative stress [17], ion channel regulation [18-

20], and metal ion distribution [21]. Structurally, when one Zn^{2+} or Cu^{2+} binds to the OR of PrP^C, a *cis*-interaction occurs between N- and C-terminus [5-8]. Due to results showing C-terminal pathological mutations weaken the Zn^{2+} and Cu^{2+}-driven *cis*-interaction [7, 8], we hypothesized that pathological mutations around the central region also weaken it. To test this hypothesis, paramagnetic relaxation enhancement NMR was used to measure the *cis*-interaction, both qualitatively and quantitatively. In contrast to C-terminal pathological mutations, this study finds that central region pathological mutations do not affect the Cu^{2+}-driven *cis*-interaction.

The importance of the metal-driven *cis*-interaction has been suggested by numerous studies. First, C-terminal pathological mutations in PrP^C have been shown to have a weakened Zn^{2+} and Cu^{2+}-driven *cis*-interaction [7, 8]. Second, ΔCR PrP^C, a designed deletion mutant that causes neonatal fatality in mice, was shown to have a weakened metal-driven *cis*-interaction [11]. Third, the interface between the metal-bound OR and the C-terminus overlap with the interface of toxic C-terminal antibodies and the C-terminus of PrP^C [5, 9]. Furthermore, the toxic effects of ΔCR PrP^C and C-terminal antibodies are dependent on the presence of the polybasic-extreme N-terminus of PrP^C [22].

The N-terminal toxicity model was then developed in which the C-terminus regulates the N-terminus by facilitating the *cis*-interaction, and when the *cis*-interaction is blocked, the N-terminus generates toxicity [11]. Spontaneous currents in electrophysiological recordings [22] as well as G418 induced toxicity in cell culture

[23, 24] have both been employed to test if a construct elicits N-terminal toxicity. It is found that central region pathological mutations (P101L, G113V, A116V, and G130V) generate these signatures for N-terminal toxicity [14, 22]. In contrast, the C-terminal pathological mutation, D177N, which can cause CJD or FFI [3], did not display spontaneous currents or G418 induced toxicity. Central region pathological mutations do not weaken the Cu^{2+}-driven *cis*-interaction, whereas C-terminal pathological mutations do [7, 8]. These results begin to suggest that central region pathological mutants drive a toxicity that is more consistent with the N-terminal toxicity model, where C-terminal pathological mutations have a different mode of toxicity that correlates with a weakening of the metal-driven *cis*-interaction [8].

What is puzzling is the fact that the GSS causing central region mutations, P101L and A116V, and the CJD causing C-terminal mutations, D177N and E199K, are all almost 100% penetrant [25]. However, both diseases, GSS and CJD, have different disease onset, symptoms, symptom duration before death, and types of plaques formed [26-28]. Perhaps central region mutations affect the way PrP^C can regulate its own N-terminus, thus driving N-terminal toxicity, and C-terminal mutations affect the metal-driven *cis*-interaction and cause toxicity through another route. Ultimately, both sets of mutations can lead to a misregulation of PrP^C, either loss or gain or exacerbation of function, which leads into aggregation and the disease state. Further investigation into the structural and functional differences between central region

and C-terminal pathological mutations will give better insight into PrP^{C}'s function and the diseased state.

References

1. Prusiner, S.B., *Prions.* Proc Natl Acad Sci U S A, 1998. **95**(23): p. 13363-83.

2. Prusiner, S.B., *The prion diseases.* Brain Pathol, 1998. **8**(3): p. 499-513.

3. Aguzzi, A., F. Baumann, and J. Bremer, *The prion's elusive reason for being.* Annu Rev Neurosci, 2008. **31**: p. 439-77.

4. Millhauser, G.L., *Copper and the prion protein: methods, structures, function, and disease.* Annu Rev Phys Chem, 2007. **58**: p. 299-320.

5. Evans, E.G., et al., *Interaction between Prion Protein's Copper-Bound Octarepeat Domain and a Charged C-Terminal Pocket Suggests a Mechanism for N-Terminal Regulation.* Structure, 2016. **24**(7): p. 1057-67.

6. Evans, E.G.B. and G.L. Millhauser, *Copper- and Zinc-Promoted Interdomain Structure in the Prion Protein: A Mechanism for Autoinhibition of the Neurotoxic N-Terminus.* Prog Mol Biol Transl Sci, 2017. **150**: p. 35-56.

7. McDonald, A.J., et al., *Altered Domain Structure of the Prion Protein Caused by Cu(2+) Binding and Functionally Relevant Mutations: Analysis by Cross-Linking, MS/MS, and NMR.* Structure, 2019. **27**(6): p. 907-922 e5.

8. Spevacek, A.R., et al., *Zinc drives a tertiary fold in the prion protein with familial disease mutation sites at the interface.* Structure, 2013. **21**(2): p. 236-46.

9. Sonati, T., et al., *The toxicity of antiprion antibodies is mediated by the flexible tail of the prion protein.* Nature, 2013. **501**(7465): p. 102-6.

10. Herrmann, U.S., et al., *Prion infections and anti-PrP antibodies trigger converging neurotoxic pathways.* PLoS Pathog, 2015. **11**(2): p. e1004662.

11. Wu, B., et al., *The N-terminus of the prion protein is a toxic effector regulated by the C-terminus.* Elife, 2017. **6**.

12. Delaglio, F., et al., *NMRPipe: a multidimensional spectral processing system based on UNIX pipes.* J Biomol NMR, 1995. **6**(3): p. 277-93.

13. Pettersen, E.F., et al., *UCSF Chimera--a visualization system for exploratory research and analysis.* J Comput Chem, 2004. **25**(13): p. 1605-12.

14. Solomon, I.H., E. Biasini, and D.A. Harris, *Ion channels induced by the prion protein: mediators of neurotoxicity.* Prion, 2012. **6**(1): p. 40-5.

15. Markham, K.A., et al., *Molecular Features of the Zn(2+) Binding Site in the Prion Protein Probed by (113)Cd NMR.* Biophys J, 2019. **116**(4): p. 610-620.

16. McDonald, A.J., B. Wu, and D.A. Harris, *An inter-domain regulatory mechanism controls toxic activities of PrP(C).* Prion, 2017. **11**(6): p. 388-397.

17. Mitteregger, G., et al., *The role of the octarepeat region in neuroprotective function of the cellular prion protein.* Brain Pathol, 2007. **17**(2): p. 174-83.

18. Huang, S., et al., *Differential modulation of NMDA and AMPA receptors by cellular prion protein and copper ions.* Mol Brain, 2018. **11**(1): p. 62.

19. Stys, P.K., H. You, and G.W. Zamponi, *Copper-dependent regulation of NMDA receptors by cellular prion protein: implications for neurodegenerative disorders.* J Physiol, 2012. **590**(6): p. 1357-68.

20. Watt, N.T., et al., *Prion protein facilitates uptake of zinc into neuronal cells.* Nat Commun, 2012. **3**: p. 1134.

21. Pushie, M.J., et al., *Prion protein expression level alters regional copper, iron and zinc content in the mouse brain.* Metallomics, 2011. **3**(2): p. 206-14.

22. Solomon, I.H., et al., *An N-terminal polybasic domain and cell surface localization are required for mutant prion protein toxicity.* J Biol Chem, 2011. **286**(16): p. 14724-36.

23. Massignan, T., E. Biasini, and D.A. Harris, *A Drug-Based Cellular Assay (DBCA) for studying cytotoxic and cytoprotective activities of the prion protein: A practical guide.* Methods, 2011. **53**(3): p. 214-9.

24. Massignan, T., et al., *A novel, drug-based, cellular assay for the activity of neurotoxic mutants of the prion protein.* J Biol Chem, 2010. **285**(10): p. 7752-65.

25. Minikel, E.V., et al., *Quantifying prion disease penetrance using large population control cohorts.* Sci Transl Med, 2016. **8**(322): p. 322ra9.

26. Collins, S., C.A. McLean, and C.L. Masters, *Gerstmann-Straussler-Scheinker syndrome,fatal familial insomnia, and kuru: a review of these less common human transmissible spongiform encephalopathies.* J Clin Neurosci, 2001. **8**(5): p. 387-97.

27. Hsiao, K., et al., *Linkage of a prion protein missense variant to Gerstmann-Straussler syndrome.* Nature, 1989. **338**(6213): p. 342-5.

28. Masters, C.L., D.C. Gajdusek, and C.J. Gibbs, Jr., *Creutzfeldt-Jakob disease virus isolations from the Gerstmann-Straussler syndrome with an analysis of the various forms of amyloid plaque deposition in the virus-induced spongiform encephalopathies.* Brain, 1981. **104**(3): p. 559-88.

CHAPTER 4

Conclusions

The prion field has been extensively researched over the past 350 years. Numerous findings, three of which have led to Nobel Prizes, have helped move forward the field by increasing the understanding of this class of diseases. However, there are still questions regarding the mechanistic and structural origin for the observed neurotoxicity in TSEs. The primary objective of this thesis is to try to understand how the Central Region (CR) of PrP^C regulates the toxic potential of the N-terminus. We initially hypothesized the CR's regulatory role over the N-terminus was to either facilitate the metal-driven *cis*-interaction or by containing the locus for α-cleavage. However, by using specific protein design, biochemistry, and cell-based assays, we discovered that neither of hypotheses is the basis for the regulation over the toxic potential of the N-terminus. Moreover, we found that the CR facilitates the dimerization potential of PrP^C. This suggests that dimerization is a mechanism that regulates the intrinsic toxic potential of the N-terminus. Structurally, it is conceivable that dimerization may position the N-terminus away from the membrane. Blocking dimerization with ΔCR PrP^C or G5 PrP^C could plausibly free up the N-terminus, allowing for membrane destabilization and cause the unregulated entry of ions into the cell. Alternatively, dimerization could prevent the N-terminus from over-activating cognate ion channels, such as the AMPAR or NMDAR.

Do these results mean that the metal-driven *cis*-interaction and α-cleavage is not important for normal PrP^C structure and function? The metal-driven *cis*-interaction occurs when PrP^C binds to one Zn^{2+} or Cu^{2+} ion. Therefore, if PrP^C's

regulation over the AMPAR and NMDAR is Zn^{2+} and Cu^{2+} dependent, respectively, then it can be suggested that the metal-driven *cis*-interaction is engaged during these regulatory roles. As for α-cleavage, it naturally occurs in healthy tissues in everyone's brain. This cleavage event in the brain generates the N1 fragment which regulates myelination in Schwann cells, which occurs in the peripheral nervous system. Selective deletion of PrP^C in the brain and not in the periphery of mice causes a demyelinating polyneuropathy, indicating that α-cleavage occurring in the central nervous system produces the biologically active N1 fragment that migrates to Schwann cells in the peripheral nervous system and regulates their myelination. In normal physiology, α-cleavage, and presumably the metal-driven *cis*-interaction, occur and seem to regulate PrP^C biology in some fashion.

Familial prion diseases are caused by point mutations within the PrP^C gene that results in a predisposition for misfolding and ultimately prion diseases. These pathological mutations typically occur in two main regions of PrP^C: 1) the structured C-terminus, and 2) the CR. Using NMR, it was previously demonstrated that a number of these familial mutations contained in the C-terminus weaken the metal-driven *cis*-interaction. Intriguingly, it was observed that these particular mutations produce a charge change from either negative to positive or negative to neutral, and typically cause CJD or FFI. In contrast to the charge reversal pathological mutations in the structured C-terminal domain, disease producing mutations in the CR do not affect

the charge of the amino acid and typically cause GSS. We have found that familial mutations in the CR do not have a weakened Cu^{2+}-driven *cis*-interaction. Therefore, it is plausible that the origin of PrP^{C} misregulation in GSS generating mutations is different than C-terminal mutations that drive. The observation we made could help enlighten the differences in the types of symptoms, symptom onset, symptom duration, and the region where neurodegeneration occurs in the brain between GSS and CJD.

Ultimately, all familial prion diseases lead to the misfolding and template-driven PrP^{Sc} propagation and subsequently death. Understanding the molecular underpinnings and the series of events that can lead to these diseases is extremely important for pursing new avenues of therapeutic intervention. Unfortunately, a cure or an effective treatment for these diseases does not currently exist. However, our results imply that there are different changes occurring between these two classes of prion diseases. Familial CJD mutations elicit an alteration to the metal-driven *cis*-interaction, where GSS mutations in the CR does not generate this change. Furthermore, gross manipulation of the CR by mutating it to a flexible glycine-serine-rich linker does not affect the metal-driven *cis*-interaction, but does still generate toxicity. Moreover, addition of an α-cleavage site within this glycine-serine rich linker does allow for α-cleavage; however, toxicity still persists. What we do observe is that the glycine-serine-rich linker, as well as ΔCR PrP^{C}, both have a reduction in

dimerization potential on the cell membrane. These results permit us to suggest that the CR may regulate the toxic potential of the N-terminus by allowing for dimerization and that the negatively-charged patch on the C-terminus facilitates the metal-driven *cis*-interaction.

Overall, the results I present in this dissertation begin to give a molecular-based inference into the differences between the origin of PrP^C misregulation in CJD and FFI when compared to GSS. More specifically, CJD and FFI mutations can lead to a weakened metal-driven *cis*-interaction and thus misregulation of the toxic N-terminus. In contrast, GSS mutations could lead to a reduction in dimerization potential of PrP^C, thus leading to a misregulated N-terminus. The results presented in this dissertation now make it possible to begin asking more specific and directed questions about the origin of neurotoxicity in the different prion diseases.